universität wien

MASTERARBEIT / MASTER'S THESIS

Titel der Masterarbeit / Title of the Master's Thesis

Leukocyte telomere length throughout the continuum of colorectal carcinogenesis

verfasst von / submitted by

Cornelia Zöchmeister, BSc MSc

angestrebter akademischer Grad / in partial fulfilment of the requirements for the degree of

Master of Science (MSc)

Wien, 2017 / Vienna 2017

Studienkennzahl lt. Studienblatt / degree programme code as it appears on the student record sheet:	A 066 834
Studienrichtung lt. Studienblatt / degree programme as it appears on the student record sheet:	Masterstudium Molekulare Biologie UG2002
Betreut von / Supervisor:	Ao. Univ.-Prof. Mag. Dr. Andrea Gsur

Table of contents

Danksagung

Mein besonderer Dank gilt meiner Betreuerin Frau Ao. Univ.-Prof. Mag. Dr. Andrea Gsur (Institut für Krebsforschung, Klinik für Innere Medizin I, Medizinische Universität Wien), die die Durchführung meiner Masterarbeit in diesem Ausmaß ermöglicht hat und durch Ihre Unterstützung zum Gelingen dieser Arbeit maßgelblich beigetragen hat.

Mein Dank gebührt auch Assoc. Prof. Priv.-Doz. Mag. Dr. Hedwig Sutterlüty-Fall (Institut für Krebsforschung, Klinik für Innere Medizin I, Medizinische Universität Wien) für die Bereitstellung des Forschungslabors und die fachliche Hilfestellung auf dem Gebiet der Zellkultur. Des Weiteren möchte ich mich bei Mag. Dr. Andreas Baierl (Department of Statistics and Operations Research, Universität Wien) für die Unterstützung der statistischen Auswertung bedanken.

Ganz besonders möchte ich mich bei meinen Kollegen Philipp und Stefanie bedanken. Danke für unsere zahlreichen Gespräche und konstruktiven Diskussionen, eure stetige Unterstützung und unser freundschaftliches Arbeitsklima. Auch bei meinen Kolleginnen Ricarda und Ines bedanke ich mich für ihre große Hilfsbereitschaft. An dieser Stelle möchte ich mich auch bei Angelina, Vanita und Jihen bedanken, die mich in diverse Arbeitsmethoden unterwiesen und mich so freundlich in die Gruppe aufgenommen haben.

Außerdem gilt mein besonderer Dank Prof. Dr. Rajiv Kumar (Deutsches Krebsforschungszentrum DKFZ, Heidelberg) für die großzügige Bereitstellung der Forschungsmöglichkeiten und die Integration in seine Forschungsgruppe. Desgleichen bedanke ich mich herzlich bei Dr. Sivaramakrishna Rachakonda (Deutsches Krebsforschungszentrum DKFZ, Heidelberg) für seine geduldige Unterweisung und permanente Unterstützung im Labor.

Darüber hinaus gebührt mein großer Dank der COST Action (European Cooperation in Science and Technology), die durch die finanzielle Unterstützung im Rahmen eines Forschungsstipendiums die Durchführung dieser Arbeit ermöglicht hat.

Nicht zuletzt möchte ich besonders meiner Familie danken, allen voran meinen Eltern und meiner Schwester Angelika für ihre moralische Unterstützung und Geduld, die während meines gesamten Studiums von unschätzbarem Wert waren.

Abstract

Considering the continuously high prevalence and relatively high mortality of colorectal cancer (CRC) on a global scale, there is a strong interest in the detection of potential clinical biomarkers in order to identify high-risk groups for CRC and therefore cast doubt on the necessity of colonoscopy for the majority of the population.
Telomeres consist of highly conserved nucleoprotein structures that cap chromosome ends and are accountable for preserving genomic stability to prevent degradation and end-to-end fusion. It is widely accepted that the progressive shortening of telomeres contributes to genomic instability and is crucially involved in the process of carcinogenesis. Telomere length is maintained by human telomerase reverse transcriptase (hTERT), its genetic variants may influence hTERT activity.

The present study investigated the functionality of MNS16A, a tandem repeat minisatellite located downstream of hTERT in a putative promoter region of a TERT antisense RNA transcript. As previous research of our molecular epidemiology group identified two new MNS16A variants, promoter activity of all six known MNS16A variable number of tandem repeats (VNTRs) was examined in colorectal cancer cell line SW480 and HCT-116. An inverse correlation between promoter activity and number of tandem repeat elements could be demonstrated, although general expression level in cell line HCT-116 was considerably lower. Further cancer epidemiological studies need to verify the potential of MNS16A genotypes as biomarker for cancer susceptibility, taking tumor-type and tissue-specific functionality as well as transcription factor binding sites and MNS16A VNTR length into account.

In the second part of this work, relative telomere length in peripheral blood leukocytes (PBL) was measured within the Colorectal Cancer Study of Austria (CORSA), involving 384 CRC cases as well as age- and gender-matched 544 high-risk adenomas, 537 low-risk adenoma patients and 546 colonoscopy-negative controls. As previous studies have found inconsistent associations between CRC and PBL telomere length as potential biomarker, this study additionally comprised premalignant precursors in order to reflect the whole spectrum of putative CRC development.

Telomeres were found to be significantly longer in CRC patients compared to control subjects (*P*-value = 3.61×10^{-6}). No significant differences in telomere length could be detected for high-risk (*P*-value = 0.05956) and low-risk colorectal adenoma patients (*P*-value = 0.05224).

Age-dependent telomere attrition was prevalent throughout the entire study population, though the decline was more pronounced in female subjects and current smokers. As a statistically significant association of longer telomeres in patients with CRC compared to colonoscopy-negative controls was found, PBL telomere length could be applied as clinical biomarker for CRC in the future. However, further large studies similarly including colorectal adenomas are necessary to confirm these results.

List of Figures

List of Tables

Abbreviations

ALT	Alternative lengthening of telomeres
Amp	Ampicillin
APC	Adenomatous polyposis coli
BES	N,N-Bis(2-hydroxyethyl)-2-aminoethanesulfonic acid
BBS	BES buffered saline
B-PREDICT	Burgenland PREvention trial of colorectal Disease with ImmunologiCal Testing
BSA	Bovine serum albumin
$CD4^+$	Cluster of differentiation 4
CFP	Cyan fluorescent protein
CIN	Chromosomal instability
CMV	Cytomegalovirus
CORSA	Colorectal Cancer Study of Austria
CRC	Colorectal cancer
Ct	Cycle threshold
DMEM	Dulbecco's modified Eagle's medium
DMSO	Dimethylsulfoxid
DNA	Deoxyribonucleic acid
E. coli	Escherichia coli
EDTA	Ethylenediaminetetraacetic acid
EMT	Epithelial-mesenchymal transition
FCS	Fetal calf serum
flow-FISH	Flow fluorescence in situ hybridization
GATA	GATA binding factor
GR	Glucocorticoid receptor
HBS	HEPES buffered saline
HEPES	4-(2-hydroxyethyl)-1-piperazineethanesulfonic acid
HP	Hyperplastic polyp
hTERC	Human telomerase RNA component
hTERT	Human telomerase reverse transcriptase

ISC	Intestinal stem cell
Kras	Kirsten rat sarcoma viral oncogene homolog
KRK	Kolorektales Karzinom
LB	Lysogeny Broth
Lgr5	Leucine-rich-repeat containing G-protein-coupled receptor 5
LOH	Loss of heterozygosity
MAPK	Mitogen-activated protein kinase
MSI	Microsatellite instability
MMQPCR	Monochrome multiplex quantitative PCR
MMR	Mismatch repair
mRNA	Messenger ribonucleic acid
NFκB	Nuclear factor Kappa B
NSCLC	Non-small cell lung cancer
NTC	No template control
OD	Optical density
PBL	Peripheral blood leukocyte
PBS	Phosphate-buffered saline
PCR	Polymerase chain reaction
PLB	Passive lysis buffer
PROSA	Prostate Cancer Study of Austria
Q-FISH	Quantitative fluorescence in situ hybridization
qRT-PCR	Quantitative real-time polymerase chain reaction
R^2	Coefficient of determination
RNA	Ribonucleic acid
RNP	Ribonucleoprotein
ROS	Reactive oxygen species
SSA	Sessile serrated adenoma
SV40	Simian virus 40
TA cell	Transit amplifying cell
TFB	Transformation buffer
TFBS	Transcription factor binding site
TFII-I	General transcription factor II-I
TP53	Tumor protein p53

TRF	Terminal restriction fragment
TSA	Traditional serrated adenoma
T/S ratio	Telomere signal/single copy gene signal ratio
VNTR	Variable number of tandem repeat
Wnt	Wingless-type mouse mammary tumor virus integration site family member
XBP	X-box binding protein

1. Introduction

1.1. Telomeres

Telomeres are highly conserved non-coding hexameric nucleotide repeat $(TTAGGG)_n$ sequences at the end of all linear eukaryotic chromosomes (Blackburn and Szostak, 1984; Moyzis *et al.*, 1988). Along with the protein complex shelterin, they form protective and highly conserved nucleoprotein structures that facilitate genomic stability and integrity (Palm and de Lange, 2008). Telomeric repeats can vary in size from 0.15 to 50 kilobases, a single-strand overhang at the 3' end forms a specific T-loop structure which stabilizes the end of chromosomes and prevents degradation and end-to-end fusion (Griffith *et al.*, 1999). The end replication problem of telomeres causes progressive shortening of telomere length accompanying cell division, usually triggering apoptosis, cellular senescence or immortalization in somatic cells (Counter *et al.*, 1992; Aubert and Lansdorp, 2008). In replicating cells, telomeres continuously shorten between 50 and 100 base pairs with each cell division due to the fact that DNA polymerases are not able to completely replicate the terminal telomeric sequences (Greider and Blackburn, 1996). When telomeres progressively shorten and become dysfunctional, this results in genomic instability including chromosome fusions, breakings or translocations. Those genetic alterations can allow selective advantage in growth for affected cells and therefore enable enhanced chance of survival and proliferation (Sharpless and Depinho, 2004). In mouse embryonic stem cells, short telomeres affected epigenetic regulation and consequently cell differentiation via decreased genome-wide DNA methylation, highlighting the importance of functional telomeres (Pucci, Gardano and Harrington, 2013). To escape replicative senescence when telomeres get critically shortened, cells have acquired mechanisms to stabilize the end of their chromosomes. The expression of the enzyme telomerase maintains and lengthens telomeres by *de novo* synthesis of telomere repeats (Bertorelle *et al.*, 2014). Additionally, alternative lengthening of telomeres (ALT) represents a telomerase-independent pathway to maintain telomere length. Homologous recombination between sister telomeres facilitates homology directed repair which can also result in highly varying telomere length (Palm and de Lange, 2008).

1.2. Telomerase

Telomeres are maintained and newly synthesized by the ribonucleoprotein (RNP) complex known as telomerase (Greider and Blackburn, 1985; Blackburn, 1992). Its human telomerase RNA component (hTERC) subunit serves as RNA template, its human telomerase reverse transcriptase (hTERT) protein subunit has telomerase reverse transcriptase activity (Feng *et al.*, 1995; Nakamura and Cech, 1998). While the activity of hTERT is generally repressed in human somatic tissues, most cancer cells as well as germ-line cells feature hTERT activity that allows continued proliferation (Kim *et al.*, 1994). Telomerase is active in embryonic cells until 20 weeks of gestation to ensure rapid tissue growth (Wright *et al.*, 1996), in adult somatic tissue only bone marrow and peripheral blood leukocytes featured detectable telomerase activity (Broccoli, Young and de Lange, 1995). Active telomerase enables extension of telomeric DNA sequences, thereby counteracting the common telomere erosion process and consequently leading to replicative immortality, a hallmark of cancer (Hanahan and Weinberg, 2011). The telomerase activity might possibly be regulated via telomere length itself, considering the distal location of hTERT gene on chromosome 5. The typical telomeric loop structure of telomeres could have a silencing effect on the expression of the hTERT gene. Only if telomeres are critically shortened, telomerase could be reactivated and TERT promoter mutations might accumulate, reflecting a possible hTERT autoregulation (Shay and Wright, 2000). Accumulation of template RNA, association with TERT and catalytic activation as well as subsequent telomere recruitment are the essential steps in the process of forming a functional telomerase holoenzyme (Collins and Mitchell, 2002). In approximately 85-90% of all cancer cases, hTERT is actively expressed (Kim *et al.*, 1994; Shay and Bacchetti, 1997; Ã and Wright, 2005; Akincilar, Unal and Tergaonkar, 2016) whereas hTERT mRNA levels are usually tightly controlled and limit telomerase reactivation under physiological conditions (Counter *et al.*, 1998). Extension and maintenance of telomeres represent the main contribution of telomerase in tumorigenesis, yet there is also evidence for its interaction with the Wnt/β-catenin (Park *et al.*, 2009) and the NFκB signaling pathway (Ghosh *et al.*, 2012). Thus, TERT is suspected to be involved not only in proliferation, but also in cellular signaling, survival and regulation of cell cycle (Perrault, Hornsby and Betts, 2005).

1.3. Telomere length in colorectal carcinogenesis

1.3.1. Telomere length in colorectal cancer tissue

Extreme alterations of telomeres are causing genomic instability, also impacting on gene expression and phenotypic heterogeneity and therefore contributing to features of tumor aggressiveness and clinical outcome (Bisoffi, Heaphy and Griffith, 2006). Declining telomere length in tumor tissue has been reported for colorectal carcinoma (CRC) in the first place (Hastie *et al.*, 1990). Further studies also confirmed that telomeres of CRC tissue exhibited significantly shorter length in comparison to healthy adjacent tissue (Takagi *et al.*, 1999; Gertler *et al.*, 2004; Garcia-Aranda *et al.*, 2006; Rampazzo *et al.*, 2010); however, inconsistency in literature arose when not all findings could ascertain telomere reduction in CRC (Katayama *et al.*, 1999). Telomere attrition was demonstrated in low- and high-grade colonic dysplasia (Raynaud *et al.*, 2008); similarly in adenoma with a diameter >2cm, telomeres were found to be significantly shorter than in adjacent and distant normal colorectal mucosa (O'Sullivan *et al.*, 2006). A telomere lengthening tendency that was found in invasive CRC compared to its premalignant precursors could potentially reflect telomerase activation and indicate that initial telomere erosion might be crucial in colorectal carcinogenesis. Telomere attrition already seems to take place in early stages during the generation of low-grade dysplasia, this trend intensifies with high-grade dysplasia. A critically short telomere length might possibly allow cells to overcome cell cycle arrest and enable continued proliferation and malignant transformation (Raynaud *et al.*, 2008). As opposed to normal mucosa where telomere length decreases with advancing age, this effect could not be observed in colorectal carcinomas (Hastie *et al.*, 1990; Gertler *et al.*, 2004; Rampazzo *et al.*, 2010). Regarding the relationship between tumor location and telomere length, telomeres were longer in rectal cancer (Rampazzo *et al.*, 2010) and shorter in tumors of the right colon (Garcia-Aranda *et al.*, 2006; Rampazzo *et al.*, 2010). Although longer telomeres were detected in advanced tumors (Engelhardt *et al.*, 1997; Gertler *et al.*, 2004), the association between telomere length and tumor stage and progression still remains unclear (Takagi *et al.*, 1999; Rampazzo *et al.*, 2010; Valls *et al.*, 2011).

1.3.2. Telomere length in peripheral blood leukocytes

Considering the continuously high prevalence and relatively high mortality of CRC globally (Ferlay *et al.*, 2013), there is a strong interest in the detection of potential clinical biomarkers.

Especially the investigation of peripheral blood leukocyte (PBL) telomere length has been focused upon in order to identify high-risk groups for CRC and therefore spare the majority of the population colonoscopy. Previous studies have found inconsistent associations between PBL telomere length and CRC so far. Three prospective case-control studies could not reveal any association of telomere length with CRC (Zee *et al.*, 2009; Lee *et al.*, 2010; Pooley *et al.*, 2010). In the retrospective SEARCH Colorectal Study (Pooley *et al.*, 2010) as well as in a retrospective case-control study within the Chinese Han population (Qin *et al.*, 2014) shorter mean PBL telomere length was associated with CRC risk. A comparably large study comprising 598 CRC patients and 2,212 healthy controls found that younger individuals with longer PBL telomeres or older individuals with shorter telomeres were associated with an increased risk for CRC (Boardman *et al.*, 2014). Similarly, in the Shanghai Women's Study findings indicated an elevated risk for CRC in the presence of very short and very long telomere length, analyzing telomere length in peripheral blood of 441 women with CRC and 549 matched controls in a nested case-control approach (Cui *et al.*, 2012). Recently, a meta-analysis by Naing et al. examined the association between PBL telomere length and CRC risk, thereby including all of the above-mentioned studies. Neither in the prospective nor in the retrospective pooled analyses, an association between PBL telomere length and CRC risk could be ascertained. As only a limited number of studies was included in this meta-analysis, the authors emphasized that there is a continued need for large well-designed studies on this topic (Naing *et al.*, 2017). In terms of overall survival and relapse-free survival, shorter PBL telomere length could be associated with worse prognosis as well as advanced tumor stages in CRC patients. In addition, higher proportion of $CD4^+$ cells and diminished B cell percentage were found in patients with short telomere length, suggesting that shortened telomeres might be involved in impaired immune status and consequently poor CRC prognosis (Chen *et al.*, 2014).

1.4. Histopathology of colorectal adenoma and cancer

Colorectal cancer (CRC) is the second most common cancer in women and the third most common cancer in men worldwide. In Austria, the incidence ranges in the top third within the European Union (Ferlay *et al.*, 2013). According to the most widely accepted model of adenoma-carcinoma sequence (Leslie, Carey and Steele, 2002), colorectal carcinomas arise from normal colorectal mucosa, the transition proceeds gradually from early benign precursor stage to advanced premalignant polyps terminating in malignant neoplasia with potential invasiveness (Bresalier RS., 2002). The histological classification of colorectal polyps is

characterized by their potential to generate neoplastic lesions. Hyperplastic polyps are considered to be non-neoplastic, whereas tubular adenomas, tubulo-villous adenomas and villous adenomas are attributed to have neoplastic capability. Depending on the degree of dysplasia, adenomas are categorized into low-grade and high-grade adenomas. The type and size of the polyp as well as the degree of dysplasia are correlated with malignancy: An increased potential of malignant transformation is linked to higher grade of dysplasia, polyp size greater than 1 cm and increasing villous proportion within the polyp. Tubular adenomas are composed of 0-25% villous tissue, tubulo-villous adenomas comprise 25-75% and villous adenomas 75-100% villous tissue. Penetration through the muscularis mucosae into the submucosa is a critical event that defines malignancy of colorectal neoplasia. The risk of developing consecutive (metachronous) advanced adenomas is related to several criteria: No medical history of CRC in the family and one to two small tubular adenomas (<1cm) are considered as low risk factors, while patients with polyps of tubulo-villous and villous histology, polyp size greater than 2 cm, multiple polyps, male gender and CRC in family history are at high risk and require a close follow-up (Colucci, Yale and Rall, 2003).

Apart from the classical adenoma-carcinoma pathway that is decisive for 50-70% of all CRC cases, the serrated pathway is held responsible for 30-35% of CRC origin. Among the serrated lesions, it can be distinguished between hyperplastic polyps (HP), sessile serrated adenomas (SSA) and traditional serrated adenomas (TSA) (Singh *et al.*, 2016). The last two adenoma types are important premalignant lesions and precursors of CRC. The occurrence of SSA and TSA is associated with similar or higher risk for CRC than for conventional adenomas (Erichsen *et al.*, 2016). Hyperplastic polyps do not give rise to CRC. However, HPs morphologically resemble SSAs which complicates accurate identification of those premalignant lesions during colonoscopy (Singh *et al.*, 2016). Regarding CRC, the vast majority (more than 90%) are classified as adenocarcinomas that originate from the colorectal epithelium (Hamilton, Bosman FT and Boffetta, 2010). The glandular formation within colorectal adenocarcinomas determines the state of differentiation and histological tumor grading: With increasing loss of gland formation, adenocarcinomas are categorized as less differentiated. Generally, a moderate differentiation is found in ~70% of diagnosed colorectal adenocarcinomas (Fleming *et al.*, 2012).

There are two putative models of CRC histopathogenesis, aiming to explain the cell origin of colorectal carcinoma: the 'top-down' model suggests that tumor initiation spreads laterally and downwards from the top of the crypt. This theory was supported by findings in spontaneous adenomas where dysplastic cells harboring an adenomatous polyposis coli (*APC)* mutation could only be found at the luminal side of the crypt (Shih *et al.*, 2001). The contrasting 'bottom-up' model proposes that transformed cells originate from crypt stem cells at the bottom of the crypt and expand to populate the entire crypt. Patients with a genetic predispostion in the *APC* gene often manifest monocryptal adenoma where entire crypts are covered by dysplastic cells (Preston *et al.*, 2003). However, those two models are not mutually exclusive and tumor initation and dedifferentiation might occur in intestinal stem cells (ISCs) expressing the stem cell marker Lgr5 (leucine-rich-repeat containing G-protein-coupled receptor 5) as well as in differentiated Lgr5-negative cells (Schwitalla *et al.*, 2013).

Intestinal stem cells (ISCs) ensure the remarkably high potential of self-renewal throughout the entire intestine. They reside in the intestinal epithelium at the bottom of each crypt and give rise to transit amplifying (TA) cells that are strongly proliferating as the main source of epithelial renewal. Due to short lifespan of differentiated epithelial cells, there is a rather low probability of accumulating mutations and potential cancer initiation originating from those cells. In case of TA cells or ISCs, they are more prone to contribute to cancer development through growth advantage acquired by a selective mutation (Huels and Sansom, 2015). ISCs as well as CRC cells share a generally high activity of Wnt/β-catenin signaling. Expression of β-catenin is associated with epithelial-mesenchymal transition (EMT) and dedifferentiation in colorectal cancer (Brabletz *et al.*, 2005). Mutations of *APC* impair regulated Wnt signaling and keep cells in a crypt-progenitor phenotype. If functional *APC* is lost, the lack of controlled β-catenin signaling is supposed to be the initiating cause of tumorigenesis (Sansom *et al.*, 2004). In mouse model, dysfunctional *APC* and aberrant nuclear accumulation of β-catenin could lead to formation of intestinal adenomas (Sangiorgi and Capecchi, 2008). Depending on the intensity of active Wnt signaling, ISCs exhibit the highest potential to initiate colorectal adenoma formation, followed by TA cells and differentiated epithelial cells (Huels and Sansom, 2015).

In addition to continued β-catenin signaling, further mutations and inflammatory signals might be necessary in cells of non-stem cell origin to drive the progression of adenomas (Westphalen *et al.*, 2014). The loss of functional *APC* itself seems not sufficient to provoke malignant transformation (Barker *et al.*, 2009); the concurrent mutation of several oncogenes and inflammation mediated via the NFκB pathway drive the Wnt signaling pathway. Loss of *APC*

combined with *Kras* mutation stimulated NFκB signaling in differentiated cells and promoted initiation of CRC. In this context, an enhanced NFκB signaling pathway is closely interconnected with the Wnt signaling pathway, both together favoring crypt-like phenotype and initiating tumor formation. In this process, intraepithelial cells of non-stem cell origin can dedifferentiate and develop tumor-initiating characteristics, cell-type plasticity enables bidirectional conversion (Schwitalla *et al.*, 2013).

1.5. Molecular genetics of colorectal tumorigenesis

The development of CRC is widely accepted to be a multi-stage process, involving several genetic as well as epigenetic steps that ultimately lead to genomic instability and a complex heterogeneity of phenotypic manifestations (Markowitz and Bertagnolli, 2009). Failure in DNA replication as well as exposure to carcinogens are suspected to represent the major cause of mutations that lead to adenoma and CRC formation (Huels and Sansom, 2015). The accumulation of chromosomal instability (CIN), microsatellite instability (MSI) and methylated CpG islands are causally involved in the initiation and progression of colorectal cancer. Genetic instability as the leading cause for tumor development in the human colon occurs in the majority of colorectal carcinoma (Pino and Chung, 2010). This genetic instability can be characterized by CIN as well as MSI. Preneoplastic alterations in colorectal tissue feature enhanced cellular proliferation, favoring the telomere shortening process. Critically shortened telomeres and telomeric dysfunction are closely linked to CIN and therefore crucially affect the transformation to cancer cells. Mutation and functional loss of tumor suppressor genes like *APC*, *SMAD 4* or *TP53* gene are consequences of chromosomal instabilities (CINs) including amplifications and translocations in colorectal cancer cells (Bertorelle *et al.*, 2014). As another result of instability at chromosomal level, mutations in *BRAF* as well as *KRAS* genes are known to exert an oncogenic effect via continued mitogen-activated protein kinase (MAPK) pathway signaling and are both supposed to contribute to tumorigenesis (Rajagopalan *et al.*, 2002). In CRC, most frequently gain-of-function mutations occur in *KRAS* (40%) and *BRAF* (10%), however their oncogenic mutations are presumed to be mutually exclusive (Morkel *et al.*, 2015). Mutated oncogenes and tumor suppressor genes can lead to loss of heterozygosity (LOH) and abnormalities of karyotype (aneuploidy), further aggravating genomic instability on the transition to colorectal neoplasia (Lengauer, Kinzler and Vogelstein, 1998).

In 65-70% of sporadic colorectal cancer cases, CIN is prominent and induces the generation of variable new karyotypes by chromosomal rearrangement, loss or gain (Lengauer, Kinzler and Vogelstein, 1998). Additionally, deficiency in DNA mismatch repair (MMR) genes generates microsatellites through unrepaired mismatched bases and thereby causes microsatellite instability (MSI) in tumor cells (Bertorelle *et al.*, 2014). Regarding clinical outcome, patients with CRC of CIN phenotype had a more unfavorable prognosis in terms of overall and progression-free survival compared to patients with MSI tumor phenotype (Walther, Houlston and Tomlinson, 2008).

Furthermore, a correlation between telomerase activity and CRC progression could be established, connecting increased hTERT expression level and consequently higher telomerase activity to poor clinical outcome (Chen and Chen, 2011). In comparison to normal colorectal tissue, an increasing trend of telomerase activity via adenoma towards carcinoma supports the adenoma-carcinoma sequence to malignant transformation (Niiyama *et al.*, 2001; Bertorelle *et al.*, 2014). Telomerase activity might also be triggered in case of *TP53* (p53*)* gene mutations (Rampazzo *et al.*, 2010) that are prevalent in almost every second CRC case, specifically even more dominant in distal and rectal carcinomas (Iacopetta, 2003). By preventing the inhibiting effect of *TP53* on TERT promoter, an active telomerase function could stabilize telomeres already at an early stage in those tumors (Rampazzo *et al.*, 2010).

1.6. Genetic variations of hTERT locus

Within the telomerase reverse transcriptase (TERT) locus several polymorphisms were reported to be associated with cancer risk, identifying the TERT gene as putative cancer susceptibility gene (Qi *et al.*, 2012; Pellatt *et al.*, 2013). TERT polymorphisms are of special interest as they may mediate telomere stabilization via telomerase activity and contribute to cancer initiation and progression. Variations on chromosome 5p15.33, the locus that harbors the TERT gene, are supposed to be involved in increasing occurrence of malignancies. Genome-wide association studies could establish a strong relation between lung cancer, basal cell carcinoma, pancreatic cancer and mutations within the coding region of TERT. As further cancer entities (bladder cancer, prostate cancer, cervical cancer and glioma) also revealed risk alleles in 5p15.33 region, this implies a causal link of TERT gene variations and tumorigenesis (Baird, 2010).

Mutations in the promoter region of TERT were frequently found in bladder cancer (59%), tumors of the central nervous system (43%), melanoma (29%) and follicular cell-derived thyroid cancer (10%) where they provoke increased telomerase expression (Vinagre *et al.*, 2013).

Relating to CRC, increased risk of colon cancer could be associated with the TERT variant rs2736118, while an inverse correlation with colon and rectal cancer was demonstrated for another TERT variant rs2853668 (Pellatt *et al.*, 2013). Further, a significant association with CRC risk was demonstrated for TERT variant rs2736098 (Jannuzzi *et al.*, 2015) as well as for TERT variant rs2736100 (Kinnersley *et al.*, 2012). A haplotype-based analysis investigated the TERT haplotypes rs2853669, rs2736100, and rs2736098 aiming to identify functional genetic variations in colorectal cancer. An association of CRC development and TERT haplotype *TGA* could be determined which showed a protective haplotype effect (Jannuzzi *et al.*, 2015). The single nucleotide polymorphism rs10936599 close to the TERC gene, encoding the RNA component of telomerase, was associated with longer telomeres in human leukocytes. The major allele at this polymorphism was further linked to increased risk for CRC and colorectal adenomas (Jones *et al.*, 2012). No association of CRC or colorectal polyps could be confirmed for individual TERT SNPs (rs2736122, rs2853676, rs2735940, rs2736098, rs2075786, rs2736100, rs4975605), only a haplotype analysis demonstrated increased risk of high-risk polyps with haplotype CGTATGG (Hofer *et al.*, 2012).

1.7. MNS16A

The polymorphic tandem repeat minisatellite termed MNS16A is located downstream of the human telomerase gene (hTERT) on chromosome 5p15.33. The hTERT gene itself consists of four exons clusters and contains several mini- and microsatellites; downstream of exon 16 the MNS16A minisatellite can be localized (**Figure 1**). This region is known to function as a putative promoter region of an antisense hTERT mRNA transcript. MNS16A minisatellite contributes to the biological function of this promoter, its activity seems to be depending on the length of tandem repeats within this minisatellite. This antisense hTERT transcript was detected only concurrently along with hTERT expression, implicating its possible regulatory role on human telomerase expression (Wang *et al.*, 2003).

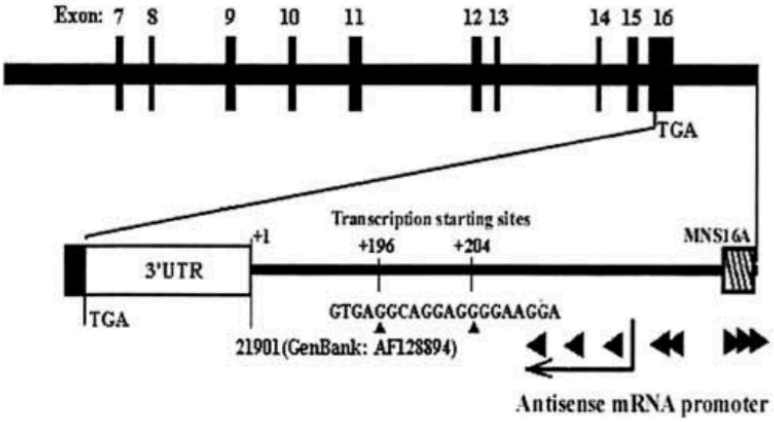

Figure 1. Core promoter of hTERT antisense transcript harboring MNS16A tandem repeat minisatellite (Wang *et al.*, 2003).

The MNS16A sequence is characterized by a core element of 23 bp tandem repeat of TCC TCT TAT CTC CCA GTC TCA TC or a 26 bp core sequence harboring a CAT trinucleotide insertion that also represents a putative binding site for transcription factor GATA-1. Different variable number of tandem repeat (VNTR) alleles were discovered that were termed according to their PCR fragment length: VNTR-212, VNTR-243, VNTR-274, VNTR-302, VNTR-333 and VNTR-364 (Wang *et al.*, 2003; Hofer *et al.*, 2011, 2013) (**Figure 2**). The number of CAT insertions increases with VNTR length. Functional analysis of VNTR-302 and VNTR-243 in a non-small cell lung cancer (NSCLC) cell line linked shorter VNTR length to higher promoter activity (Wang *et al.*, 2003). A possible explanation could be the different number of CAT insertions, thus the 26 bp core sequence including the putative GATA-1 binding site could have a repressive function on the promoter activity, inhibiting antisense hTERT mRNA transcription. However, the biological role of this antisense transcript is not fully understood so far (Jin *et al.*, 2011).

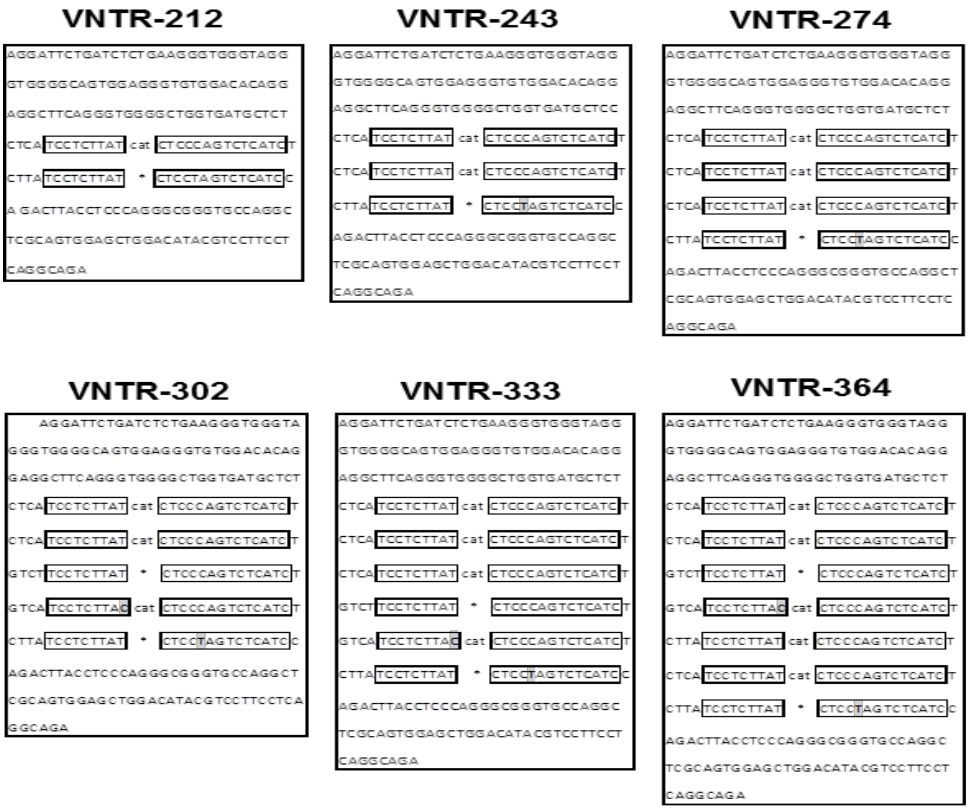

Figure 2. MNS16A variable number of tandem repeats. CAT trinucleotide insertions are flanked by core sequences (framed sequences)(Hofer *et al.*, 2011, 2013).

1.7.1. MNS16A and cancer risk

The longest MNS16A variant VNTR-364 (Hofer *et al.*, 2011) as well as the shortest VNTR-212 (Hofer *et al.*, 2013) were both identified by our research group for the first time. In order to establish genetic models and assess associated cancer risk to predict cancer susceptibility, some studies categorized MNS16A genotypes into short (S) and long (L) alleles (LS classification system), depending on the number of tandem repeats and respectively the VNTR length. VNTRs with a length of 212 bp, 243 bp and 274 bp were considered as short alleles (S), whereas alleles consisting of 302 bp, 333 bp and 364 bp were assigned to the long allele (L) category. This allowed further distinction between SS, LS or LL genotype groups. Additional differentiation into a LMS classification system determined another middle allele (M) category, including the 274 bp allele (Hofer *et al.*, 2011; Jin *et al.*, 2011; Xia *et al.*, 2013).

In our Colorectal Cancer Study of Austria (CORSA), Hofer et al. reported that this medium length allele VNTR-274 could be linked to CRC. As a 2.7-fold increased risk was associated with this allele in comparison to the wild-type allele VNTR-302, the middle allele VNTR-274 could possibly present a risk factor for CRC (Hofer *et al.*, 2011). The MNS16A-S allele was correlated with an enhanced cancer susceptibility to tumors of the central nervous system (malignant gliomas) (Carpentier *et al.*, 2007). A cumulative analysis of five cerebral cancer studies, including the afore mentioned study, confirmed the significant association of MNS16A short allele with risk of cerebral cancer. Furthermore, a pronounced association between breast cancer risk and MSN16A (LS vs. LL genotype) was determined, while for lung cancer no statistically significant relationship could be established. According to the LMS classification, short allele (S) showed an increased cancer risk in all genetic models compared to the middle allele (M) of MNS16A (Xia *et al.*, 2013).

2. Aim of the study

The activity of human telomerase reverse transcriptase (hTERT) is considered to maintain telomere length and enable replicative immortality. Therefore, more detailed knowledge of genetic variants that influence hTERT activity is of particular interest. Within the scope of this work the promoter activity of all known MNS16A variable number of tandem repeats (VNTRs) was examined in two colorectal cancer (CRC) cell lines. Investigating the functionality of this polymorphic tandem repeat minisatellite that is located within a putative promoter region of a regulatory element of hTERT contributes to the understanding of genetic polymorphisms associated with CRC risk.

Telomere length is a crucial factor for genomic stability and cell survival. Both extremely shortened as well as elongated telomeres lead to genomic instability and might cause the cell to undergo apoptosis or initiate neoplastic progression. Telomere dysfunction and crisis are known to be involved in development of CRC. The length of telomeres is affected by multiple environmental and genetic factors which all have an impact on telomere homeostasis. Assuming that telomere length is critical for the onset of colorectal carcinoma, alterations of telomere length in the tumor tissue as well as in peripheral blood may have important implication as potential biomarker. Hence, in the second part of this work peripheral blood leukocyte (PBL) telomere length was measured in a study population that included patients with CRC, high-risk and low-risk adenoma as well as colonoscopy-negative controls, reflecting the continuum of colorectal carcinogenesis. The length of telomeres in peripheral blood may carry clinical information as it might indicate the progress of colorectal malignancy. A possible relationship between PBL telomere length and occurrence of CRC could allow the applicability of PBL telomere length as biomarker to asses CRC risk.

3. Material and Methods

3.1. Molecular Biology Methods

3.1.1. Plasmid vectors

MNS16A VNTR constructs had been inserted in the backbone of the pGL3-basic vector (Promega, Madison, WI, USA). This vector contained a Firefly Luciferase reporter gene but lacked eukaryotic promoter and enhancer sequences. The pGL3-basic vector itself was used as promoterless negative control. The pGL3 CMV vector contained a constitutively active cytomegalovirus (CMV) promoter and served as a positive control. The pRL-SV40 Renilla Luciferase Control Reporter Vector (Promega) was used as an internal control reporter to express Renilla luciferase after co-transfection with experimental reporter vectors (containing Firefly Luciferase). The pAdlox CFP reporter vector was used as control reporter to visualize effective transfection upon light excitation of the cyan fluorescent protein (CFP). An overview of plasmid vectors is depicted in **Table 1**. Schematic diagrams of vectors are shown in Appendix A1 **(Figure 17-26)**.

Table 1. Plasmid vectors used for transfection

plasmid vector	**source**
pGL3-basic Firefly Luciferase Reporter Vector (promoterless)	Promega (Product Number E1751)
pGL3_MNS16A VNTR constructs	Institute of Cancer Research, Medical University of Vienna, Dr. Andrea Gsur research group
pGL3 CMV	Institute of Cancer Research, Medical University of Vienna, Dr. Hedwig Sutterlüty-Fall research group
pRL-SV40 Renilla Luciferase Control Reporter Vector	Promega (Product Number E2231)
pAdlox CFP	Institute of Cancer Research, Medical University of Vienna, Dr. Hedwig Sutterlüty-Fall research group

3.1.2. Transformation into competent Escherichia coli XL-1

For the preparation of competent E. coli, XL-1 bacteria were plated on agar plates (**Table 3**) without selection (containing no antibiotics) and grown overnight (37°C). A single colony was picked and inoculated in 2.5ml LB medium (amp^-, 180rmp, 37°C, overnight) (**Table 3**). This bacterial culture was then diluted (1:100) with 250ml LB medium (amp^-) and 5ml 1M $MgSO_4$. The culture was kept at 37°C (180rpm, 3-4 hours) until the optical density (OD_{600nm}) had reached a value between 0.4 and 0.6. Bacteria were pelleted by centrifugation for 5 minutes at 4500g at 4°C. The pellet was resuspended in 100ml ice cold TFB1 buffer (**Table 2**). Bacteria were chilled on ice for 5 minutes and again pelleted using centrifugation at the same conditions (5 minutes, 4500g, 4°C). Pellets were resuspended in 10ml ice cold TFB2 buffer (**Table 2**) and incubated for 60 minutes on ice. Competent bacteria were aliquoted and stored at -80°C.

Table 2. Buffers for transformation into competent Escherichia coli XL-1

TFB1 buffer	**TFB2 buffer**
30mM CH_3COOK	10mM MOPS
10mM $CaCl_2$	75mM $CaCl_2$
50mM $MnCl_2$	10mM RbCl
100mM RbCl	15% glycerol
15% glycerol	
Adjusted to pH 5.8 with CH_3COOH	Adjusted to pH 6.5 with 1M KOH

Table 3. LB (Lysogeny Broth) medium and agar

LB medium:	10g/l tryptone (pancreatic digest of casein)
	5g/l yeast extract
	5g/l NaCl
20g/l of LB-Broth (Sigma-Aldrich, St. Louis, Missouri, USA) were filled up with ddH_20 and autoclaved. Alternatively before use, 1µl ampicillin (100µg/ml) per 1ml LB medium was added.	
LB agar:	15g/l agar
	10g/l tryptone
	5g/l yeast extract
	5g/l NaCl
35g/l of LB-Agar (Sigma-Aldrich) were filled up with ddH_20 and autoclaved. 1µl ampicillin (100µg/ml) per 1ml LB agar was added before pouring the warm agar into petri dishes.	

3.1.3. Cesium chloride density gradient centrifugation

Plasmid vector DNA was purified by cesium chloride density gradient centrifugation. This method facilitated to yield high-quality plasmid DNA of pGL3_MNS16A VNTR constructs as well as pGL3-basic, pGL3 CMV, pRL-SV40 and pAdlox CFP vector.

Competent XL-1 Escherichia coli bacteria were transformed with plasmid vector DNA (**Table 1**). 100µl of competent XL-1 bacteria were incubated with 1µl DNA on ice (20 minutes), kept in water bath (at 42°C for 90 seconds) and again on ice (2 minutes). Transformed E. coli were plated on agar plates containing ampicillin (100µg/ml). After overnight incubation at 37°C, a single colony was inoculated in 3ml LB medium (amp^+) and then overnight in 400ml LB medium (amp^+) at constant agitation (180 rpm, 37°C). Cultures were pelleted by sequential centrifugation steps (5000rpm, 5min, 20°C; SORVALL RC6 centrifuge; Thermo Electron Corporation, Massachusetts, USA). Bacterial pellets were resuspended in 15ml LB medium (amp^+) and centrifuged at 10 000 rpm for 10 minutes at 20°C.

After short-term storage at -20°C, recovered pellets were dissolved by vortexing with 1ml cold sucrose solution (25% w/v, **Table 4**). For bacterial lysis, 200µl lysozyme solution (1% w/v), 400µl 0.25M EDTA solution (pH 8), 1.6 ml Triton X-100 Lytic Mix solution (**Table 4**) were sequentially added and mixed with the pellets and incubated on ice. Bacterial cells were centrifuged (16 000rpm, 30 minutes, 4°C), the resulting supernatant was transferred into a 15ml falcon, containing 5.33 g cesium chloride for a concentration of 0.97g/ml (AppliChem GmbH, Darmstadt, Germany) and filled up with TES buffer (**Table 4**) to a final volume of 5.5ml. Two sequential ultracentrifugation steps were performed (55 000 rpm, 22 hours, 14°C) in an Optima L-100 XXP centrifuge using NVTI 65-2 rotor (Beckman Coulter GmbH). Ethidium bromide (100µl and 75µl each) was added to Quick-Seal tubes (Beckman Coulter GmbH, Brea, USA) and filled with bacterial cesium chloride solution. The lower DNA band was drawn off twice with a needle (18G) and a syringe. The DNA solution was filled up to 6ml with T/E buffer (pH 8, **Table 4**). Isoamyl alcohol was used to extract the ethidium bromide. DNA precipitation was performed by adding one-tenth volume of sodium acetate (3M, pH 5.2), the 2.5-fold volume of ice cold ethanol (100%) and overnight incubation at -20°C. DNA was pelleted (13 000rpm, 15 minutes, 4°C) and dissolved in an adequate volume of T/E buffer (pH 7, **Table 4**) to reach a final DNA concentration of approximately 500ng/µl.

DNA was measured on a Nanodrop spectrometer (NanoDrop ND-1000 spectrophotometer, PEQLAB Biotechnologie GmbH, Erlangen, Germany) at 260nm to verify DNA concentration. The ratio of the absorbance at 260 and 280 nm was used to assess the purity of DNA, values around ~1.8 were considered as pure for DNA. Samples were additionally run on an agarose gel (1%) to visualize the amount of DNA (**Chapter 3.1.4.**). Cesium chloride purification for all plasmids was carried out twice to guarantee that results were independent of the DNA purification procedure.

Table 4. Solutions and buffers for cesium chloride density gradient centrifugation

TES buffer:	0.25M EDTA pH 8
	1M Tris/HCl pH 8
	5M NaCl
Triton X-100 Lytic Mix:	0.25M EDTA pH 8
	1M Tris/HCl pH8
	10% Triton
25% sucrose solution:	sucrose
	0.25M EDTA pH 8
	1M Tris/HCl pH 8
T/E buffer pH 7 (8):	1mM EDTA pH 7 (8)
	10mM Tris/HCl

3.1.4. DNA electrophoresis

For DNA electrophoresis, PeqGold Universal Agarose (PEQLAB Biotechnologie) was dissolved in 1x TAE buffer (**Table 5**). Samples were mixed with 6x DNA loading dye (**Table 5**). 5µl pre-stained marker (HindIII/EcoRI digested Lambda DNA; Fermentas International Inc., Burlington, Canada; **Table 5**) was additionally added to every gel. Electrophoresis was run for 1 hour at 80-100V. The gel was incubated in an ethidium bromide solution (final concentration 0.25µg/ml in 1x TAE; ethidium bromide stock solution 10mg/ml, AppliChem). The banding pattern of the gel was checked in a GelDoc detection system (Bio-Rad Laboratories, Hercules, CA, USA) under ultraviolet light.

Table 5. DNA electrophoresis

50x TAE stock solution:	0.5M EDTA pH 8
	Tris base
	Glacial acetic acid
DNA loading dye (6x):	40% sucrose
	24% urea
	0.25% xylene blue
	0.25% bromphenol blue
Lambda (λ) marker:	λ-DNA (Fermentas International Inc., Burlington, Canada)
	HindIII (Roche Applied Science, Upper Bavaria, Germany)
	EcoRI (Roche Applied Science, Upper Bavaria, Germany)

3.1.5. Restriction digest

To verify purification of correct plasmids, restriction digestion of DNA yielded from cesium chloride density gradient centrifugation was performed. The restriction enzymes HindIII and KpnI were used to control for the corresponding MNS16A VNTR variant. Specification of other control digestions are shown in **Table 6**.

Table 6. Restriction digests of experimental plasmids

Vector DNA	Restriction enzymes	Buffer	Digestion
pGL3_MNS16A VNTR-364	HindIII, KpnI	2	Double digestion
pGL3_MNS16A VNTR-333	HindIII, KpnI	2	Double digestion
pGL3_MNS16A VNTR-302	HindIII, KpnI	2	Double digestion
pGL3_MNS16A VNTR-274	HindIII, KpnI	2	Double digestion
pGL3_MNS16A VNTR-243	HindIII, KpnI	2	Double digestion
pGL3_MNS16A VNTR-212	HindIII, KpnI	2	Double digestion
pGL3-basic	HindIII, BamHI	B	Double digestion
pGL3 CMV	MluI, XbaI	H	Double digestion
pRL-SV40	HindIII, BamHI	B	Double digestion
pAldox CFP	BamHI, EcoRI	B	Double digestion
pAdlox CFP	SfiI	M	Single digestion

250ng DNA were digested by adding 2µl of the respective 10x buffer (Buffer 2, New England BioLabs; Buffer B/H/M, Roche Applied Science; **Table 6**), 1µl 10x BSA (Roche Applied Science), 0.3µl of each enzyme (Roche Applied Science) and ddH_20 to reach a final volume of 20µl. Digestion was facilitated by incubating the mixture for 1 hour on a thermoblock at 37°C (or 50°C for SfiI digestion). 4µl of 6x DNA loading dye were added to the digested samples before loading on an agarose gel (1.2%). 5µl of marker (λ-DNA, HindIII/EcoRI digested) were loaded to identify the length of fragment sizes (**Chapter 3.1.4.**).

3.1.6. Isolation of peripheral blood leukocyte DNA

Genomic DNA of peripheral blood leukocytes had been purified from whole blood using a QIAamp DNA Blood Midi Kit (Qiagen, Hilden, Germany). DNA had been diluted in buffer AE (Qiagen) and stored at -80°C. The quality and quantity of DNA was measured by a Nanodrop spectrometer (NanoDrop ND-1000 spectrophotometer, PEQLAB Biotechnologie) based on the ratio of absorption at 260nm and 280nm. Only DNA samples with a ratio close to 1.8 (considered as "pure" for DNA) were included for telomere length measurement.

3.1.7. Telomere length measurement (qRT-PCR)

Monochrome multiplex quantitative PCR (MMQPCR) experiments were performed to determine relative telomere length in peripheral blood leukocytes. Experiments were conducted in a high-throughput 384-well plate format (ViiA 7 instrument, Applied Biosystems, Foster City, CA, USA). Relative telomere length was determined by applying an adapted version of a previously described protocol for telomere length measurement using qPCR (Cawthon, 2009). Reactions were carried out in triplicates in an optical 384-well reaction plate. The same plate was used to measure telomere sequences (T) as well as the albumin gene (single copy gene, S). Two sequential Real-Time PCR programs were used to generate both signals from the same well, corresponding to the same amount of DNA. Standard curves were generated separately for the telomere (T) as well as for albumin (S) products. Unknown telomere fragments (T) and albumin gene (S) of samples were quantified using the respective standard curves. Relative T/S ratios were calculated and indicated relative average telomere length. A DNA pool of 30 CORSA control patients (involving all age groups) served as reference DNA to generate standard curves for telomere and albumin runs. For standard curves, a serial dilution (1:2) of this reference DNA was prepared to yield seven standards with concentrations ranging from 50 ng to 0.78 ng.

Test samples were used at a final concentration of 5-10 ng/μl. In each approach, four primers (Sigma-Aldrich; **Table 7**) were used to amplify the telomere sequences as well as the albumin gene. Primer concentrations for telomere amplification were set to 200 nM for Telg and 400 nM for Telc. For albumin amplification 200 nM albugcr2 and 400 nM albdgcr2 were applied. The telomere primer pair was specially designed to generate a primer extension product of fixed length (79bp).

Table 7. Oligonucleotide primer sequences

Primer	**Sequence**
Telg	ACACTAAGGTTTGGGTTTGGGTTTGGGTTTGGGTTAGTGT
Telc	TGTTAGGTATCCCTATCCCTATCCCTATCCCTATCCCTAACA
Albugcr2	CGGCGGCGGGCGGCGCGGGCTGGGCGGCCATGCTTTTCAGCTCTGCA AGTC
Albdgcr2	GCCCGGCCCGCCGCGCCCGTCCCGCCGAGCATTAAGCTCTTTGGCAAC GTAGGTTTC

One single fluorescent DNA-intercalating dye Syto 9 (Life Technologies, Carlsbad, CA, USA) was used at a final concentration of 3 μM. 5X HOT FIREPol Probe qPCR Mix Plus with ROX (Solis BioDyne, Tartu, Estonia) was used as master mix reagent. Genomic DNA from test samples/standards (1.75 μl volume) and 8.0 μl of reaction mix were dispensed onto 384-well plates. No template controls (NTCs) without any genomic DNA were included in the assay to verify the specificity of the primers and any possible contamination. For each sample, triplicates of T/S ratios were independently quantified and averaged, expressing the relative telomere length.

<u>Real-time PCR conditions for telomere gene:</u>

95°C/15 min – 1 cycle

95°C/20 sec; 49°C/1 min – 2 cycles

85°C/20 sec; 59°C/30 sec (signal acquisition) – 25 cycles

<u>Real-time PCR conditions for albumin gene and melt curve analysis:</u>

95°C/15 sec; 85°C/30 sec; 84°C/30sec (signal acquisition) – 35 cycles

95°C/15 sec, 60°C/1 min (continuous signal acquisition at 0.05°C/sec ramping); 95°C/15sec

3.2. Cell biology methods

3.2.1. Cell lines

Established human colorectal cell lines (**Table 8**) were obtained from the American Type Culture Collection ATCC (Rockville, MD, USA):

Table 8. List of utilized cell lines

Cell line	ATCC definition	Tissue	Cell type	Disease
Caco-2	ATCC® HTB-37	Colon	Epithelial	Colorectal adenocarcinoma
WiDr	ATCC® CCL-218	Colon	Epithelial	Colorectal adenocarcinoma
DLD-1	ATCC® CCL-221	Colon	Epithelial	Dukes' Type C, Colorectal adenocarcinoma
HCT-116	ATCC® CCL-247	Colon	Epithelial	Colorectal carcinoma
SW480	ATCC® CCL-228	Colon	Epithelial	Dukes' Type B, Colorectal adenocarcinoma
SW620	ATCC® CCL-227	Colon, derived from metastatic site: Lymph node	Epithelial	Dukes' Type C, Colorectal adenocarcinoma

3.2.2. Tissue culture

All cell lines were cultured in a humidified 7.5% CO_2 atmosphere at 37°C in a cell incubator (Heracell™ 150 incubator, Thermo Electron Corporation). Cells were kept in culture dishes (100x20mm mm; Becton, Dickinson and Company, Franklin Lakes, NJ, USA) in Dulbecco's modified Eagle's medium (DMEM; Sigma-Aldrich) supplied with 10% fetal calf serum (Gibco®, Life Technologies), 100 IU/mL penicillin and 100 µg/mL streptomycin. Only Caco-2 cells were kept in DMEM containing 20% fetal calf serum (FCS). Cell passaging was carried out after washing cells with phosphate-buffered saline (PBS) and adding trypsin/EDTA (**Table 9**). Detached cells were resuspended in fresh medium and transferred into a new culture dish. Cells were regularly monitored for confluency and physiological conditions under an inverted phase-contrast microscope (Olympus Corporation, Tokio, Japan). For long-term storage in liquid nitrogen, cells were pelleted (800rpm, 5 minutes, 20°C) and aliquots of cells were frozen in fetal calf serum containing 10% DMSO (AppliChem).

Table 9. Phosphate-buffered saline and trypsin

10x PBS:	137mM NaCl
	2.7mM KCl
	4.3mM $Na_2HPO_4 \cdot 2\ H_2O$
	1.4mM KH_2PO_4
trypsin:	0.1% trypsin
	0.01% EDTA
	0.001% phenolred

3.2.3. Transfection

Transient calcium phosphate transfection was applied to facilitate uptake of plasmid DNA into the cells. Plasmid vector DNA was prepared by cesium chloride density gradient centrifugation.

3.2.3.1. Transfection efficiency – cyan fluorescent protein (CFP)

In initial experiments, all cell lines were transfected with pAdlox CFP vector to verify optimal transfection conditions and best suitable cell lines. A defined number of cells were seeded in 60x15mm culture dishes (between 100 000 and 180 000 cells per dish, depending on the size and growth rate). A Bürker-Türk counting chamber was used to determine the cell number. Different transfection conditions were tested in various approaches (**Table 10**).

Table 10. Transfection conditions tested for transfection of pAdlox CFP vector DNA

Buffer	**Amount of transfected DNA**	**Calcium chloride**	**Glycerol shock**
240µl 2x HBS	10µg	30µl 2M $CaCl_2$	Yes
240µl 2x HBS	10µg	30µl 2M $CaCl_2$	No
250µl BBS	10µg	25µl 2.5M $CaCl_2$	Yes
250µl BBS	10µg	25µl 2.5M $CaCl_2$	No

Table 11. 2x HBS (HEPES buffered saline) buffer for calcium phosphate transfection

2x HBS buffer:	250mM NaCl
	10mM KCl
	1.5mM $Na_2HPO_4 \cdot 2\ H_2O$
	12mM dextrose
	50mM HEPES (4-(2-hydroxyethyl)-1-piperazineethanesulfonic acid)
Adjusted to pH 7.05 with 0.5M NaOH, filled up with autoclaved ddH_20, filter-sterilized (0.45µm)	

Table 12. BBS (BES buffered saline) buffer for calcium phosphate transfection

BBS buffer:	BES (N,N-Bis(2-hydroxyethyl)-2-aminoethanesulfonic acid
	1M NaCl
	50mM Na_2HPO_4
Adjusted to pH 6.95 with 0.5M NaOH, filled up with autoclaved ddH_20, filter-sterilized (0.45µm)	

Table 13. Glycerol for glycerol shock

15% glycerol:	glycerol
	1x HBS buffer
For 50ml 15% glycerol solution: 7.5g glycerol weighed and filled up to 50ml with 1x HBS buffer	

For transfection procedure, DNA was diluted with water, then supplemented with $CaCl_2$. The DNA-$CaCl_2$ solution was added dropwise to the same total volume of the respective phosphate transfection buffer (2x HBS or BBS; **Table 11-12**) while simultaneously generating air bubbles (aeration) to form a fine precipitate. The transfection solution was then incubated for 20 minutes at room temperature, incubated 30 seconds on the medium-free cells before adding again the same conditioned medium. Cells were incubated overnight at 37°C and 7.5% CO_2 (or 3% CO_2 for BBS buffer). For a glycerol shock (three to five hours after transfection), 15% glycerol (**Table 13**) was added onto medium-free cells, incubated at 37°C with 7.5% CO_2 for 30 to 60 seconds. Cells were washed with 1xPBS, supplied with fresh medium and incubated overnight at 37°C with 7.5% CO_2. The medium was exchanged 24 hours after transfection and CO_2-buffered medium was added. In case of excessive precipitate, cells were washed with 1x PBS. All cells were incubated at 37°C with 7.5% CO_2 until the third day after transfection, where efficiency of transfection was determined. Using a fluorescence microscope (Eclipse TE300 inverted microscope, Nikon, Tokio, Japan) enabled the visualization of effectively transfected cells through excitation of transfected cyan fluorescent protein (CFP). The DAPI filter set was used to capture the emission of this reporter protein. Exposure time was set to 3000ms for fluorescence and 7ms for phase contrast imaging. The MetaMorph® Microscopy Automation & Image Analysis Software (Molecular Devices, Sunnyvale, CA, USA) was used along with the 18.0 Monochrome W/O IR camera (Nikon) to generate phase contrast and fluorescence images. Cell lines with a sufficient proportion of fluorescent cells were selected for further co-transfection of experimental MNS16A VNTR variants and pRL-SV40 (Renilla) vector to perform Luciferase assay.

3.2.3.2. Transfection of MNS16A VNTR variants

Colorectal cancer cell lines were transfected with six different experimental MNS16A variants in order to determine their effect on promoter activity through Luciferase assay. The day before transient calcium phosphate transfection, a defined number of cells were seeded in 60x15mm culture plates (180 000 cells per plate for HCT-116, 150 000 cells per plate for SW480). Besides the experimental pGL3_MNS16A VNTR variants, a positive control (pGL3 CMV), a negative control (pGL3-basic) and a blank transfection (containing no DNA) were included in every transfection approach. As a co-transfection was performed, pRL-SV40 vector (containing Renilla Luciferase) was transfected along with all other plasmid vectors (containing Firefly Luciferase) (**Table 14**).

Table 14. Co-transfection of experimental reporter and internal control

	HCT-116	**SW480**
pGL3_MNS16A VNTR/ pGL3-basic/ pGL3 CMV	8.5µg	10 µg
pRL-SV40 vector	1µg	3µg
Total amount of DNA	9.5µg	13µg

In the transfection approach of positive control pGL3 CMV, only 1µg of actual pGL3 CMV vector DNA was used, the remaining amount was compensated with pGL3-basic vector DNA. Previous transfection experiments with pAdlox CFP vector DNA found BBS buffer along with no glycerol shock to be the best transfection condition. The amount of buffer and calcium chloride were adapted to the respective amount of transfected DNA (**Table 15**).

Table 15. Transfection protocol

	BBS	**2.5M $CaCl_2$**	**Plasmid DNA**	**ddH_20**
HCT-116	237.5 µl	23.75µl	1µg pRL-SV40 vector (≅ 2µl) 8.5µg experimental reporter (≅ 17µl)	194.75µl
SW480	325µl	32.5µl	3µg pRL-SV40 vector (≅ 6µl) 10µg experimental reporter (≅ 20µl)	266.5µl

The transfection procedure was performed according to the protocol of transfecting pAdlox CFP vector DNA. Cells were transfected 24 hours after seeding. Cell culture medium was exchanged the next day, cells were harvested three days following transfection to monitor promoter activity in a Luciferase Assay.

3.2.4. Luciferase Assay

A Dual-Luciferase Reporter Assay System Kit (Promega, Product Number E1910) was used to measure MNS16A promoter activity in cell line SW480 and HCT-116. This assay was based on co-transfection of two individual reporter enzymes that were simultaneously expressed within the same cells. Renilla Luciferase (pRL-SV40 vector) served as an internal control reporter and functioned as baseline response. Firefly Luciferase (pGL3 vector) was used as an experimental reporter to monitor the effect of experimental conditions.

Active cell lysis was performed the third day after transfection. Cells were washed twice with 3ml 1x PBS. 400µl 1x PLB (passive lysis buffer; **Table 16**) were dispensed on the culture dish and cells were detached using a cell scraper. The cell lysate was transferred to a tube, followed by two cycles of freezing in liquid nitrogen and thawing in water bath (37°C). Cell debris was pelleted by centrifuging for 30 seconds in a Heraeus PICO 17 centrifuge (Thermo Fisher Scientific, Massachusetts, USA). 20µl supernatant were transferred into each well of a white Opaque OptiPlateTM-96 Microplate (PerkinElmer, Massachusetts, USA).

Table 16. Reagents for Luciferase Assay (provided by Dual-Luciferase Reporter Assay System Kit, Promega).

Luciferase Assay reagents	
1x PLB (passive lysis buffer):	Diluted from 5x PLB with distilled water
LAR II (Luciferase Assay Reagent II):	Lyophilized Luciferase Assay Substrate was resuspended in 10ml Luciferase Assay Buffer II and protected from light
1x Stop and Glo® Reagent:	50x Stop and Glo® Substrate were diluted with Stop and Glo® Buffer to a final 1x concentration and protected from light

100µl of LAR II (**Table 16**) were added to each well and quickly mixed with the lysate by pipetting. Chemiluminescence signals of Firefly Luciferase activity were measured on a Synergy HT Multi-Mode Microplate Reader (BioTek Instruments, Inc., Vermont, USA). 100µl of 1x Stop and Glo® Reagent (**Table 16**) were dispensed to every well and mixed with the containing solution to quench the Firefly luminescence signals and quantify Renilla Luciferase activity. Endpoint measurements of luminescence were performed after a 10-second integration time for each well.

Luminsecence signals of untransfected cells were used as blank values. For each approach, lysates were measured in duplicates. Blank values were accordingly subtracted from both Renilla as well as experimental Firefly Luciferase values. Firefly Luciferase/Renilla Luciferase ratios were calculated for each approach, normalizing Firefly to the respective Renilla values. For further normalization, those ratios were divided by pGL3 CMV Firefly/Renilla values (positive control) in order to determine relative promoter activities. For each cell line, four independent co-transfection experiments were included, using plasmid DNA from two independent cesium chloride purification procedures. Following normalization to Renilla values and pGL3 CMV (Firefly/Renilla ratio), values were averaged.

3.3. Design of the study cohort

Patients were involved within the ongoing Colorectal Cancer Study of Austria (CORSA) that has been recruiting more than 14,000 participants (mainly Caucasians) since 2003. In cooperation with the province-wide screening program "Burgenland Prevention Trial of Colorectal Disease with Immunological Testing" (B-PREDICT), individuals with positive fecal occult blood testing (FOBT) result are invited to undergo a complete colonoscopy and take part in CORSA at the time of examination. Further CRC patients have been recruited at the Medical University of Graz (Department of Internal Medicine), the Medical University of Vienna (Department of Surgery) and in three other Viennese hospitals. Blood sample collection and questionnaires assessing anthropometric and demographic factors were obtained at the time of colonoscopy. Written informed consent was given by all participants and the study was approved by the institutional review boards.

Participants were grouped according to their most severe histological finding: colorectal cancer (CRC), high-risk adenoma, low-risk adenoma or colonoscopy-negative control. The high-risk adenoma group included patients diagnosed with at least one of the following high-risk adenomas: adenomatous tubular-polyp >1cm, adenomatous tubulo-villous polyp, adenomatous villous polyp, sessile serrated adenoma (SSA) and traditional serrated adenoma (TSA). The low-risk adenoma group involved patients with adenomatous tubular polyp <1cm as most severe histological finding. In the control group, patients had never exhibited any of those polyps or any other colorectal pathological findings in their medical recording. Patients were stratified according to their age at time of blood sampling, coinciding with their most severe histological finding. Strata of five year intervals were formed ranging from the age of 40 to 90. Sample selection was performed on the basis of age and gender matched groups.

3.4. Statistical analysis

Statistical analysis was performed by Dr. Andreas Baierl (University of Vienna, Department of Statistics and Decision Support Systems) with the statistical software R version 3.33 (R Core Team, 2017. R: A language and environment for statistical computing, 2017).

3.4.1. MNS16A promoter activity

All relative promoter activity values were transformed to logarithmic scale. Regression analysis was performed with VNTR length as an indicator for relative log promoter activity. Regression models were selected according to the highest regression coefficient R^2 and their *P*-values. The replicate (experiment) itself was considered as categorical variable and was taken into account for the selection of the best regression model. Significance test as well as confidence intervals were generated for the regression model and the regression coefficients. *P*-values <0.05 were considered to reach statistical significance. Paired t-test was applied to verify any differences in mean relative log promoter activity between two different MNS16A VNTR variants.

3.4.2. Telomere length measurement

Multiple linear regression models were established to estimate an association between relative telomere length and the co-variables histological status, sex, age and smoking status. Age served as continuous covariate; histological status, gender and smoking status functioned as categorical predictors. The assumptions of linear regression were assessed by diagnostic plots. Descriptive statistics of confounding factors were derived per histological status. Apart from main effects, significant two-way interactions between predictors were tested. All tests were two-sided and *P*-values less than 0.05 were considered statistically significant.

4. Results

4.1. MNS16A promoter activity

4.1.1. DNA purification of MNS16A constructs

250ng DNA of each MNS16A construct were digested with HindIII and KpnI in a double digestion to verify that the correct MNS16A constructs were purified. Digested DNA fragments were separated by ethidium bromide stained 1.2% agarose gel. Pre-stained marker (HindIII/EcoRI digested Lambda DNA) was used as DNA standard to check DNA fragment length (**Figure 3**). The backbone of pGL3-basic vector could be detected at the length of around 4900 bp. MNS16A VNTRs were visualized according to their fragment length (consistent with their construct name) below the shortest standard DNA fragment.

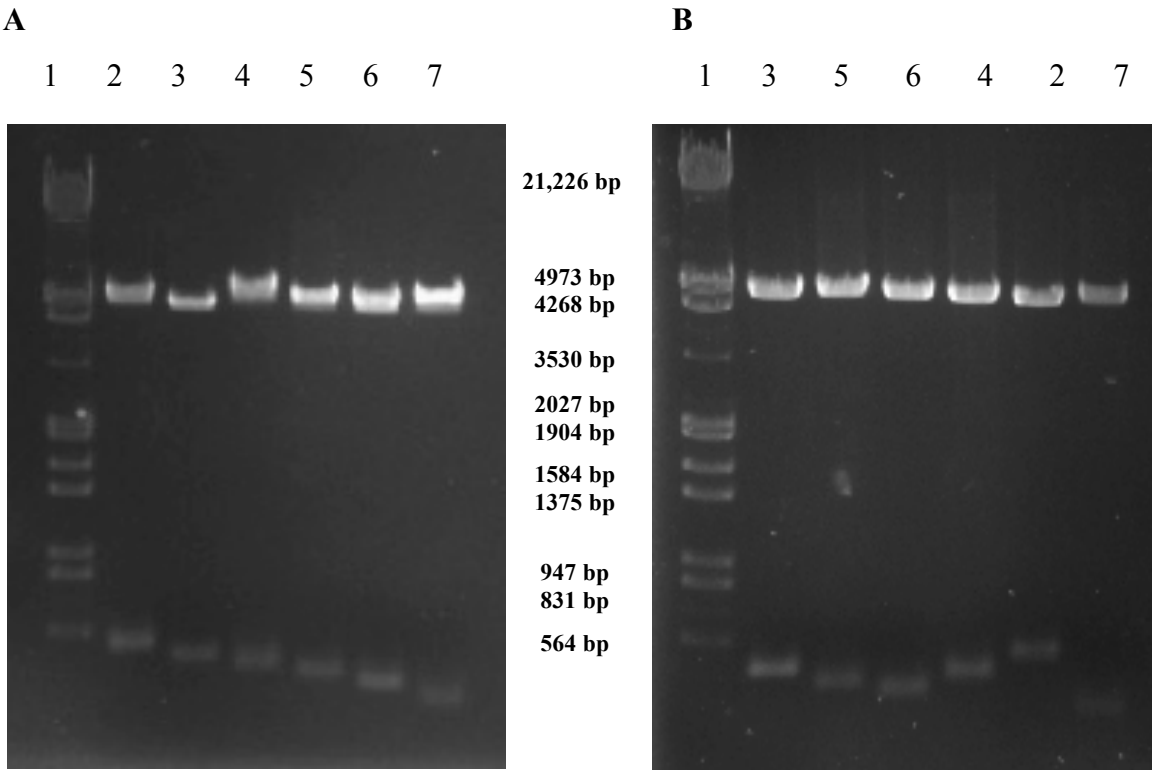

Figure 3. Restriction digest of purified MNS16A constructs of first (**A**) and second (**B**) cesium chloride purification. Samples were loaded onto the agarose gel in the following order: Lambda (λ) marker (1), VNTR-364 (2), VNTR-333 (3), VNTR-302 (4), VNTR-274 (5), VNTR-243 (6), VNTR-212 (7).

To verify equal amount of DNA in all samples, banding pattern was checked in an ethidium bromide stained 1.0% agarose gel (**Figure 4**). Upper banding demonstrated linear/nicked DNA and ranged around 5000 bp, whereas the lower band represented the supercoiled form of DNA that could be used to effectively transfect cells and was found at approximately 3500 to 4000 bp. The actual length of those DNA constructs (actual vector sizes) were 5260 bp (VNTR-364), 5214 bp (VNTR-333), 5183 bp (VNTR-302), 5155 bp (VNTR-274), 5124 bp (VNTR-243) and 5075 bp (VNTR-212). Signal strength was similar among all pGL3_MNS16A VNTR constructs, thus same DNA concentrations for all constructs could be concluded.

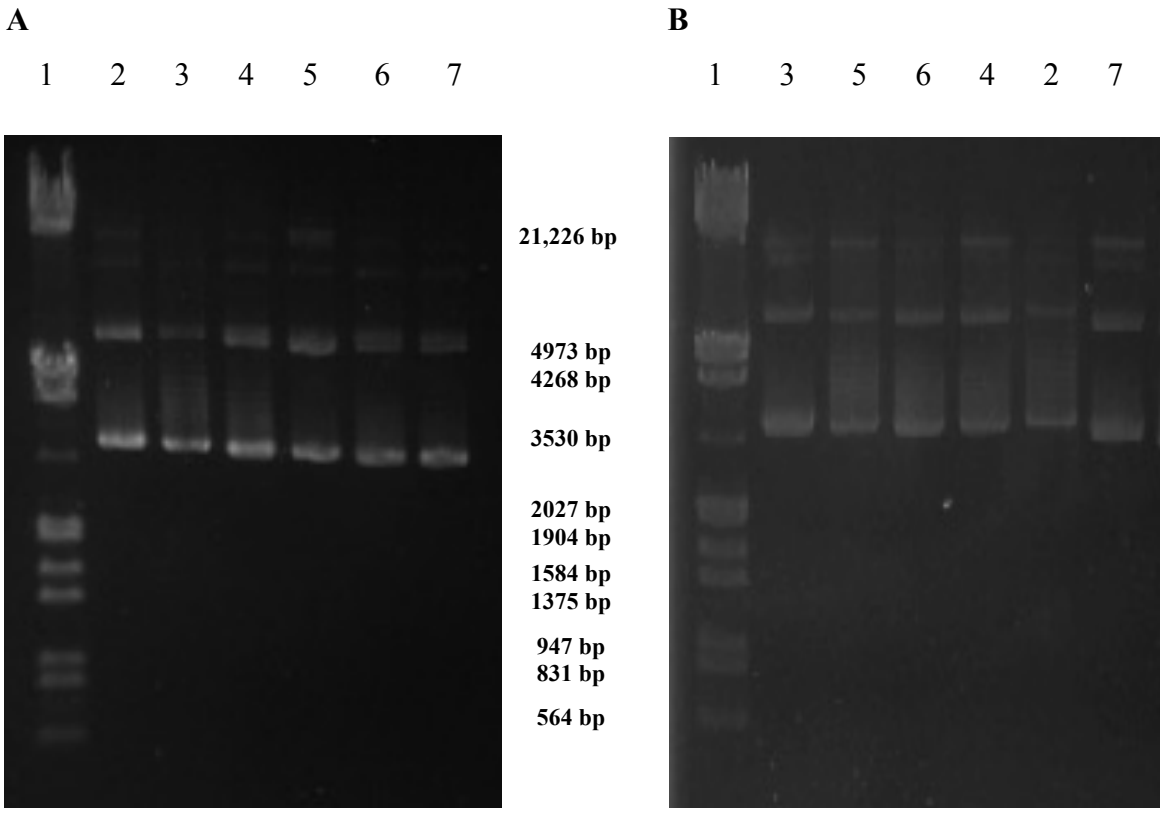

Figure 4. Purified MNS16A constructs of first (**A**) and second (**B**) cesium chloride purification. Samples were loaded onto the agarose gel in the following order: Lambda (λ) marker (1), VNTR-364 (2), VNTR-333 (3), VNTR-302 (4), VNTR-274 (5), VNTR-243 (6), VNTR-212 (7).

4.1.2. Determination of transfection efficiency

Verification of transfection efficiency was accomplished by transfection of pAdlox CFP vector. Four different transfection approaches were applied in order to find best transfection conditions. Among all tested cell lines (**Table 8**) the colorectal carcinoma cell lines HCT-116 and SW480 were figured out to exhibit the best transfection efficiency. Using 10µg DNA, BBS (BES buffered saline) buffer and no glycerol shock showed best results for HCT-116 (**Figure 5**) as well as for SW480 cells (**Figure 6**). In those two cell lines, most fluorescent cells could be detected in the fluorescence microscope three days after transfection of cyan fluorescent protein. By comparing phase contrast and fluorescent images, the corresponding proportion of fluorescent cells could be estimated. Those preliminary experiments were conducted to yield best transfection conditions and suitable cell lines that were applied to further transfection experiments of functional analysis of MNS16A tandem repeat minisatellite.

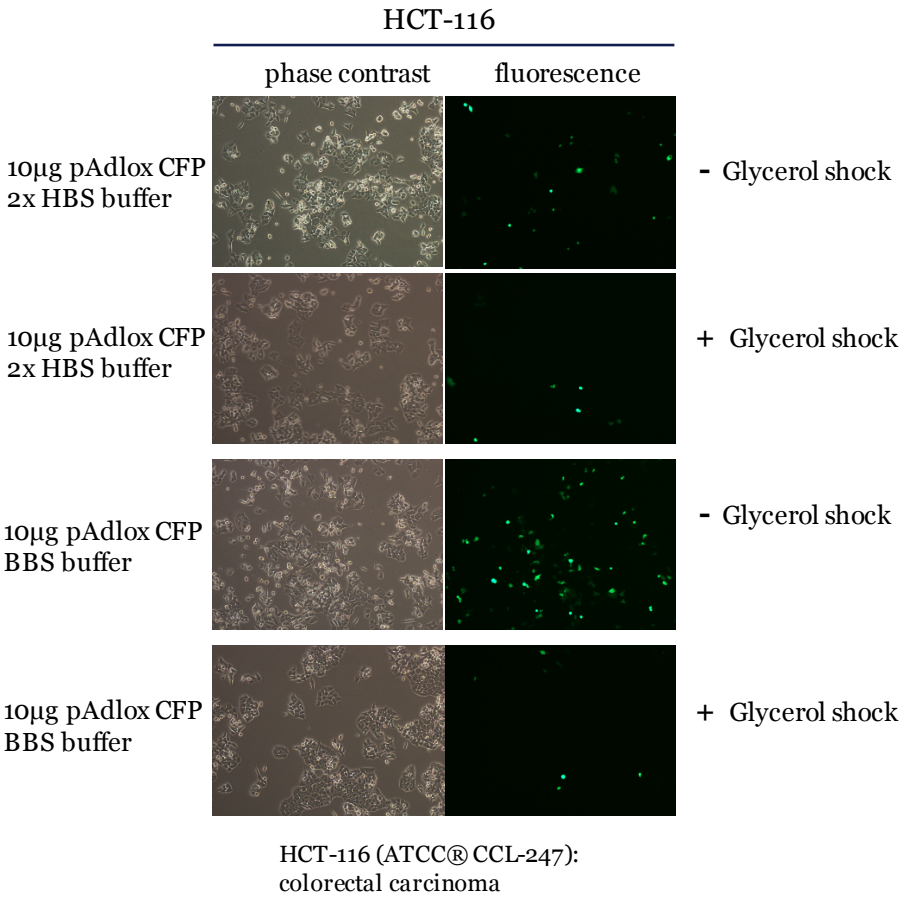

Figure 5. Phase contrast and fluorescence images of pAdlox CFP-transfected HCT-116 cells. Fluorescence image of 10µg pAdlox CFP/BBS buffer/- glycerol shock clearly featured the most fluorescent cells. Matching phase contrast and fluorescent images display the same image section.

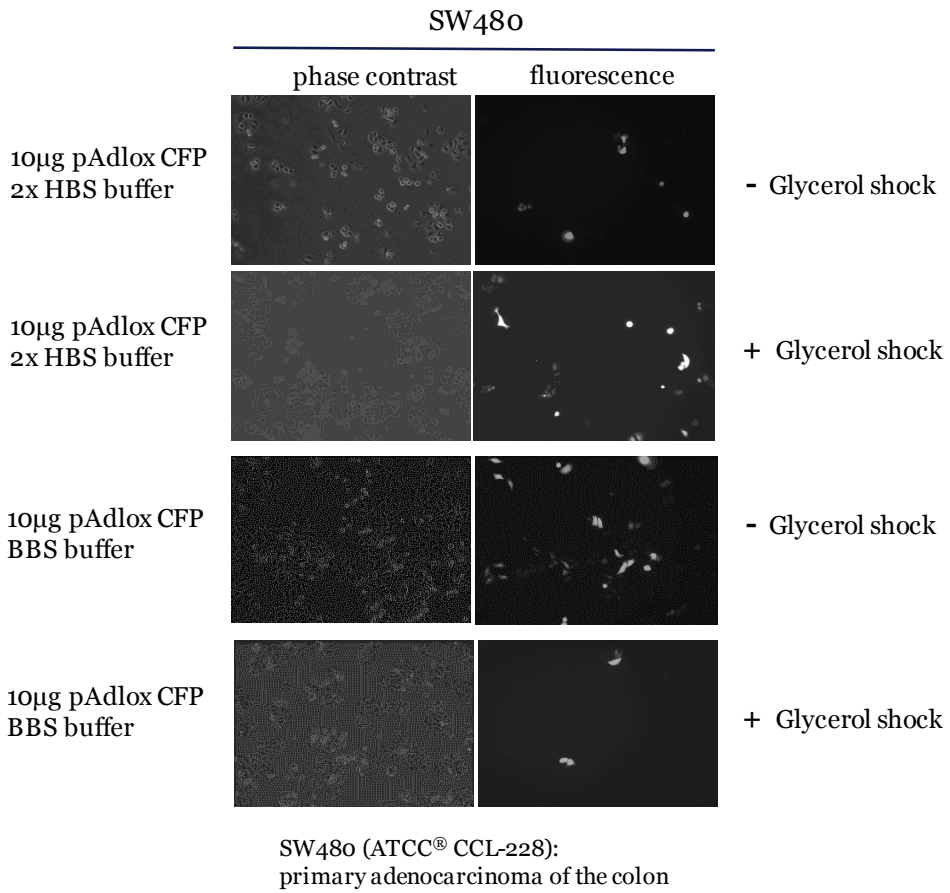

Figure 6. Phase contrast and fluorescence images of pAdlox CFP-transfected SW480 cells. Fluorescence image of 10µg pAdlox CFP/BBS buffer/- glycerol shock clearly featured the most fluorescent cells. Matching phase contrast and fluorescent images display the same image section.

4.1.3. Functional analysis of MNS16A tandem repeats minisatellite

Further Luciferase experiments were conducted for cell lines were Firefly Luciferase luminescence signals of cells transfected with pGL3 CMV exceeded a value of 100 000. Although CFP transfection experiments with cell line CCL-221 seemed to show a promising result, those cells failed to yield useful results in the Luciferase assay experiment. Only cell line HCT-116 and SW480 proved to be applicable.

Distribution of relative promoter activity of all six MNS16A VNTRs was plotted in a boxplot diagram. VNTR length was displayed on x-axis versus log transformed relative promoter activities on y-axis. Luminescence measurements were performed in duplicates, mean values and standard deviation of four independent experiments are shown.

Blank values were subtracted accordingly and Firefly/Renilla Luciferase ratios were normalized to CMV promoter positive control. Relative promoter activity on log scale enabled to visualize data in a more symmetric distribution.

4.1.4. Functional analysis of MNS16A in cell line SW480

In cell line SW480, apart from VNTR-364, all other MNS16A VNTRs showed promoter activity, significantly higher than the negative control pGL3-basic (**Figure 7**). Comparing relative promoter activity of pGL3 with VNTRs-212, -243, - 274, -302, -333, -364 on log scale, the following *P*-values were determined: 8.7×10^{-4}, 1.3×10^{-4}, 8.1×10^{-4}, 6.8×10^{-4}, 1.2×10^{-4}, 0.22. For this reason, only VNTRs that demonstrated significant relative promoter activity were considered for the regression model; VNTR-364 was not included in this cell line. In order to find the best suitable type of relationship between VNTR length and relative promoter activity, linear and linear piecewise regression models were evaluated (**Table 17**).

For the linear regression model, a significant negative trend could be identified (*P*-value = 0.00599). Regarding the coefficient of determination (R^2), it demonstrated to be slightly higher for the linear piecewise model ($R^2 = 0.77252$) than for the simple linear model ($R^2 = 0.74293$). However, the difference between those two models was not statistically significant (*P*-value = 0.19860). Consequently, the simple linear regression model was the most appropriate to describe the negative linear correlation of VNTR length and promoter activity and was chosen as best model fit (**Figure 8**). It showed a trend of increasing promoter activity for decreasing VNTR length (inverse correlation). Furthermore, paired t-tests could not find a significant difference between selected MNS16A VNTRs (**Table 18**).

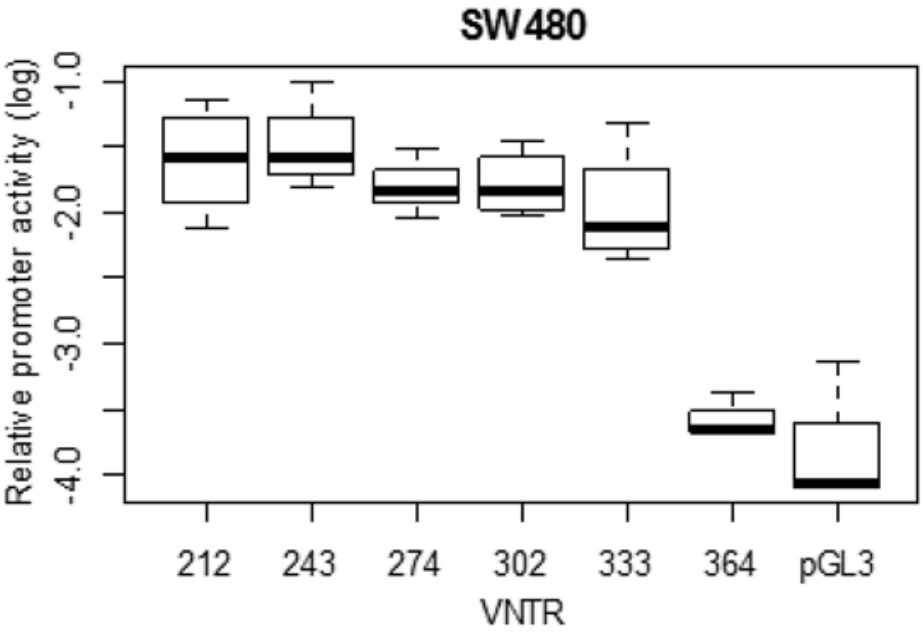

Figure 7. Relative promoter activity of different MNS16A VNTRs in cell line SW480 determined by Luciferase reporter assay.

Table 17. Linear and linear piecewise regression models for cell line SW480 (model coefficients)

Linear regression	
R^2 linear trend	0,74293
Linear slope	-0,00340
P-value linear slope	**0,00599** **
Piecewise regression	
R^2 piecewise	0,77252
P-value linear vs. piecewise	**0,19860**
Estimated breakpoint	222,95395
Slope left	0,01456
Slope right	-0,00482
P-value slope left	0,29377
P-value slope right	0,00567

Table 18. Paired t-tests for cell line SW480

	VNTR length	
paired t-tests	212 vs 243	-0,11498
	P-value 212 vs 243	0,47477
	243 vs 274	0,30668
	P -value 243 vs 274	0,07706
	274 vs 302	-0,01834
	P -value 274 vs 302	0,79456
	302 vs 333	0,19336
	P -value 302 vs 333	0,16839

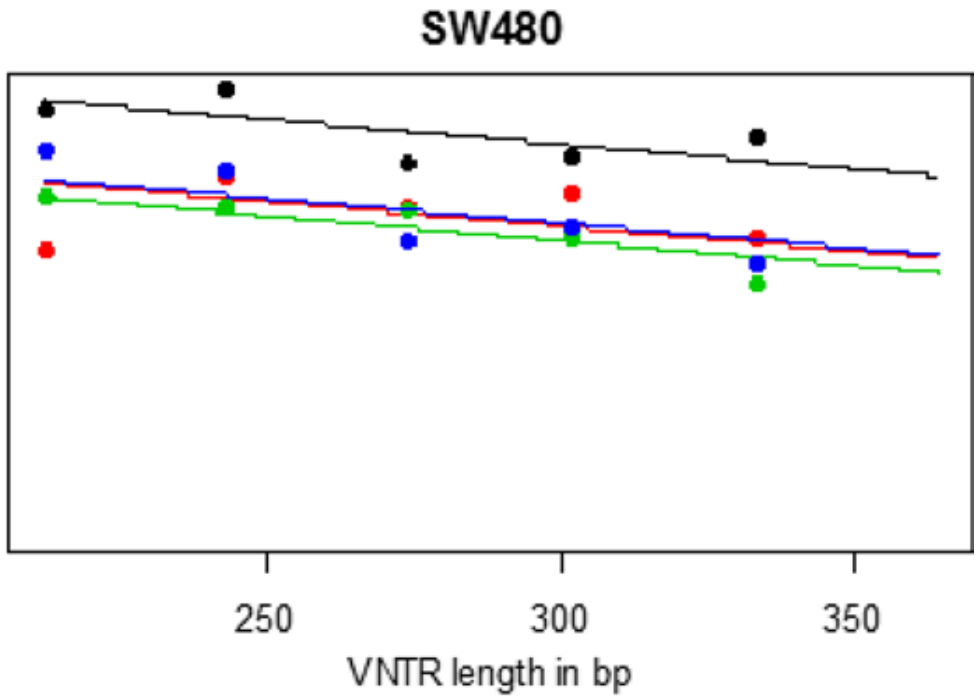

Figure 8. Linear regression model of relative promoter activity (x-axis) of MNS16A VNTRs in cell line SW480. Four independent experiments are depicted by graph lines.

4.1.5. Functional analysis of MNS16A in cell line HCT-116

For cell line HCT- 116, only the two shortest VNTR-212 and VNTR-243 demonstrated relative promoter activity higher than the negative control pGL3-basic (**Figure 9**). When comparing VNTRs-212, -243, - 274, -302, -333, -364 log values with pGL3 log values, the following *P*-values were obtained: 1.3 x 10^{-4}, 0.024, 0.98, 0.56, 0.36, 0.017. Although VNTR-364 also demonstrated a *P*-value below 0.05, its promoter activity seemed to be significantly lower than pGL3 and therefore exhibited no measurable promoter activity. Exclusively VNTR-212 and VNTR-243 showed promoter activity significantly differing from negative control, concluding that those signals were not a background noise. Regression analysis in order to assess a possible association between promoter activity and length of MNS16A VNTR failed for this cell line. Therefore, no best model fit could be estimated. Due to missing regression model, in **Figure 10** only dots are shown, representing individual measurements. Paired t-tests determined significant differences between several MNS16A VNTRs (**Table 19**). However, none of those differences in promoter activity could contribute to describe a meaningful relationship between VNTR length and promoter activity.

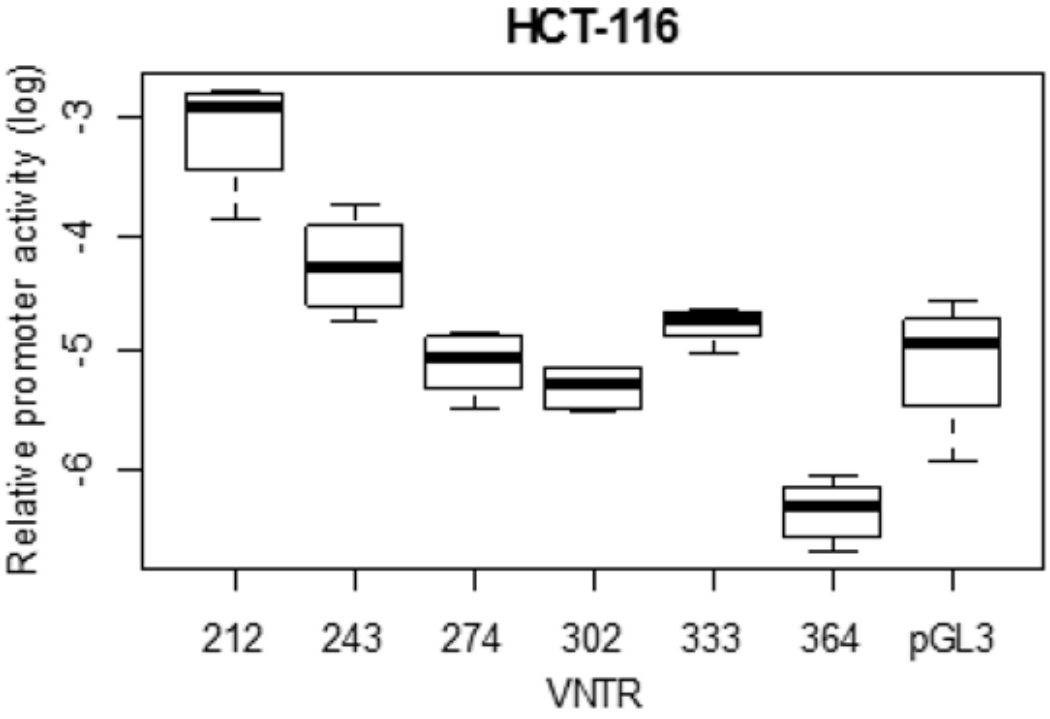

Figure 9. Relative promoter activity of different MNS16A VNTRs in cell line HCT-116 determined by Luciferase reporter assay.

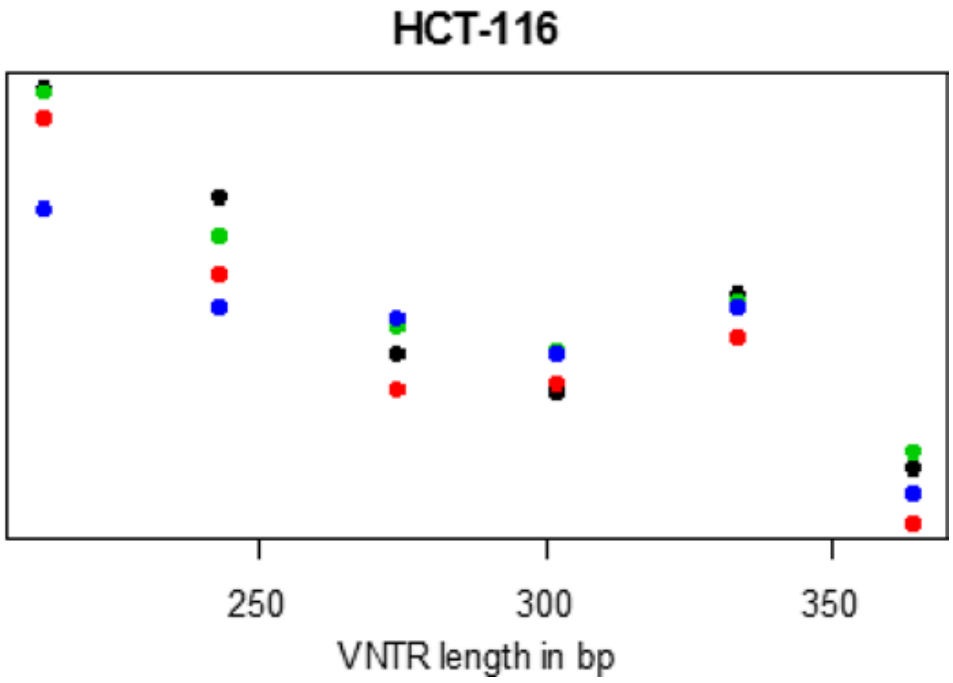

Figure 10. Missing regression model of relative promoter activity (x-axis) of MNS16A VNTRs in cell line HCT-116. Four independent experiments are depicted by differently colored dots.

Table 19. Paired t-tests for cell line HCT-116

	VNTR length	
paired t-tests	212 vs 243	1,16390
	P-value 212 vs 243	0,00281 **
	243 vs 274	0,83817
	P-value 243 vs 274	0,05999
	274 vs 302	0,21177
	P-value 274 vs 302	0,12722
	302 vs 333	-0,54712
	P-value 302 vs 333	0,01943 *
	333 vs 364	1,59904
	P-value 333 vs 364	0,00022 ***

4.2. Telomere length measurement

4.2.1. Study population

The study population consisted of 2006 individuals, 40% female (796 of 2006) and 60% male (1210 of 2006). In total, 546 colonoscopy-negative control patients, 383 patients with colorectal carcinoma (CRC), 542 high-risk adenoma patients and 535 low-risk adenoma patients were included for further analysis. In proportion to the colorectal carcinoma group, 1.4-fold more patients were involved in the control and the adenoma groups. The majority of patients could be assigned to the age groups between 50 and 80 years. Missing values of smoking status emerged from missing questionnaire data. In **Table 20** characteristics of the study population are presented, relative values refer to distribution within each group.

Table 20. Study population: distribution of cases and controls according to sex, age and smoking status

		Controls	**CRC**	**High-Risk**	**Low-Risk**	***P*-value** (differences between status groups)
	N	546	383	542	535	0,9981
Sex	F	217 (40%)	151 (39%)	215 (40%)	214 (40%)	0,9725
Age	≤ 40	11 (2%)	8 (2%)	10 (2%)	9 (2%)	
	≤ 50	36 (7%)	29 (8%)	37 (7%)	38 (7%)	
	≤ 60	134 (25%)	86 (22%)	132 (24%)	132 (25%)	
	≤ 70	152 (28%)	111 (29%)	150 (28%)	159 (30%)	
	≤ 80	180 (33%)	120 (31%)	186 (34%)	182 (34%)	
	≤ 90	33 (6%)	29 (8%)	27 (5%)	15 (3%)	
Smoking	current	57 (10%)	54 (14%)	116 (21%)	93 (17%)	0,00001 ***
	former	163 (30%)	91 (24%)	174 (32%)	159 (30%)	
	never	309 (57%)	129 (34%)	233 (43%)	265 (50%)	
	missing	17 (3%)	109 (28%)	19 (4%)	18 (3%)	

4.2.2. Relative telomere length

Relative telomere length was expressed as ratio between telomere signals (T) and single copy gene signals (S), yielding a relative T/S ratio. Normalization was accomplished on two levels: Within each unknown sample, telomere signals were related to single copy gene signals, creating T/S ratios. In addition, T/S ratio of pooled standard DNA was used as a reference for calibration. The T/S ratio of individual unknown samples had to be normalized with the T/S ratio of this reference DNA. For each sample, triplicates of T/S ratios were independently quantified and averaged. Samples with a cycle threshold (Ct) standard deviation above 0.5 were omitted from the analysis and repeated in an independent experiment. PCR efficiency was calculated based on the slope of the curve, according to the following equation:

$$E = -1 + 10^{\left(-\frac{1}{slope}\right)}$$

Efficiency for both amplicons ranged between 97-105 %. In each run, triplicates of standard samples (reference DNA) were included twice. This allowed to monitor the intra-plate as well as the inter-plate variation. Intra-plate variation for telomere signals (T) was found to be ≤ 1.9% and ≤ 0.9% for single copy gene signals (S). Inter-plate variation ranged around 5.0% for telomeric repeats and around 1.9% for albumin gene (**Appendix A2**, **Figure 27-28**). Samples with an average T/S ratio greater than 2.5 were not included in the study population (5 of initially 2011 were not considered for analysis) (**Figure 11**).

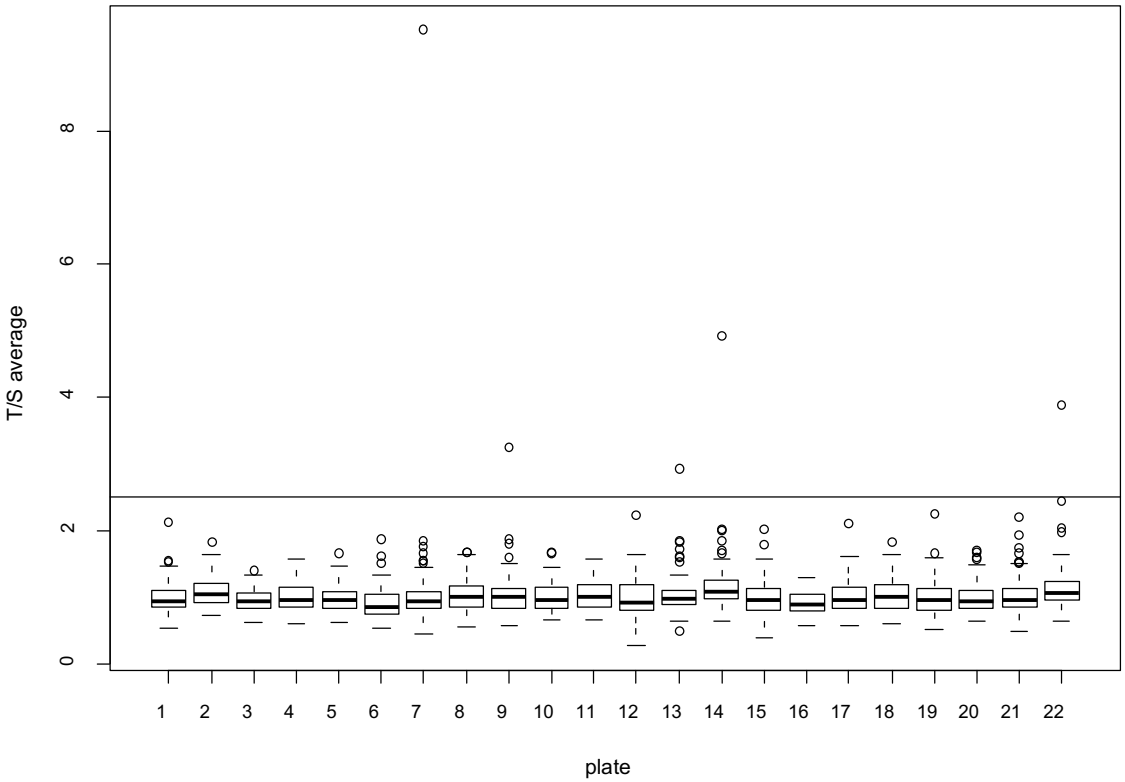

Figure 11. Distribution of average T/S ratios among measurement plates.

To evaluate the effect of status (most severe histological finding) and co-variates (age, sex, smoking status) on relative telomere length, several regression models were tested. For all regression analyses, the colonoscopy-negative control group, female sex and current smoking status were used as reference categories.

Considering only the effect of the most severe histological finding on relative telomere length, patients with colorectal carcinoma (CRC) demonstrated to have longer telomere length compared to colonoscopy-negative subjects (*P*-value = 0.014, **Table 21**).

Table 21. Effect of status on relative telomere length

Model: status only				
	Estimate	**Std. Error**	**t value**	**Pr(>|t|)**
(Intercept)	0.98865	0.01058	93.423	<2e-16 ***
status CRC	0.04054	0.01649	2.458	0.014 *
status HR	0.02156	0.01501	1.436	0.151
status LR	0.02374	0.01505	1.578	0.115

In the best suitable multiple linear regression model, the effect of explanatory (independent) variables (histological finding, age, sex, smoking status) on relative telomere length as dependent variable was considered (**Table 22**). Due to missing smoking data, 163 patients were excluded from regression analysis.

Table 22. Best model for effect of independent variables and selected interactions on relative telomere length

Best Model: status + age, sex, smoking + interactions sex, smoking with age (163 with missing smoking excluded)

Coefficients:

	Estimate	**Std. Error**	**t value**	**Pr(>|t|)**
(Intercept)	0.980710	0.021214	46.229	$< 2 \times 10^{-16}$ ***
status CRC	0.079773	0.017166	4.647	3.61×10^{-6} ***
status HR	0.026909	0.014274	1.885	0.05956 .
status LR	0.027596	0.014207	1.942	0.05224 .
Age	-0.012486	0.001487	-8.398	$< 2 \times 10^{-16}$ ***
Sex Male	-0.051949	0.011790	-4.406	1.11×10^{-5} ***
Former smoker	0.015836	0.019358	0.818	0.41344
Never smoker	0.048524	0.018723	2.592	0.00963 **
Age:Sex Male	0.001750	0.001095	1.597	0.11033
Age:former smoker	0.003296	0.001603	2.055	0.03998 *
Age:never smoker	0.003370	0.001514	2.226	0.02613 *

Signif. codes: 0 '***' 0.001 '**' 0.01 '*' 0.05 '.' 0.1 ' ' 1

Residual standard error: 0.229 on 1832 degrees of freedom

Multiple R-squared: 0.1564, Adjusted R-squared: 0.1518

F-statistic: 33.97 on 10 and 1832 DF, *P*-value: < 2.2e-16

Inverse correlation between relative telomere length and age

As expected, average T/S ratios were inversely associated with age among all status groups, though no interaction between cases and controls could be observed (**Figure 12; Appendix A3, Table 23**). Straight lines depicted in the scatterplot ran in parallel and did not intersect. The following linear equations demonstrate the declining trend of T/S ratio with increasing age:

- CON: 1.754 - 0.0119 * Age
- CRC: 1.882 - 0.0126* Age
- HR: 1.867 - 0.0132 * Age
- LR: 1.798 - 0.0121 * Age

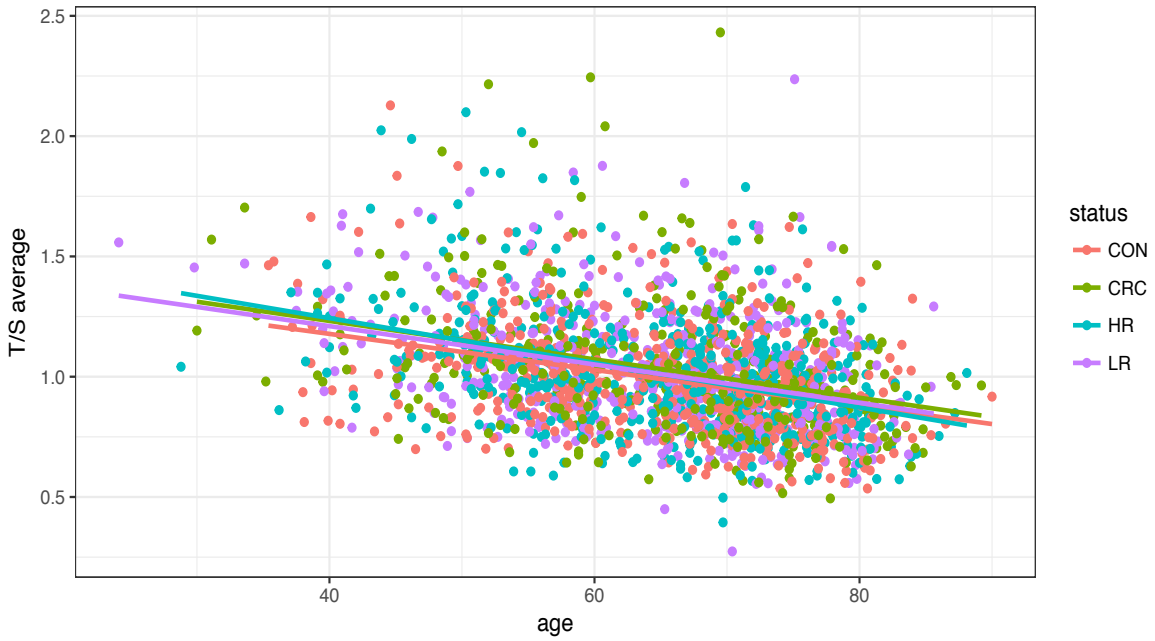

Figure 12. Association between age and relative telomere length (CON – control, CRC – colorectal carcinoma, HR – high-risk adenoma, LR – low-risk adenoma).

Regarding sex, the accelerated telomere shortening with age was more pronounced in female than in male subjects (**Figure 13**). Although female patients showed higher T/S ratios at younger age, telomere length seemed to converge to average male T/S ratios over time (*Male*: 1.628 - 0.0107 * Age; *Female*: 1.754 - 0.0119 * Age). However, in the regression analysis this interaction between age and sex did not reach statistical significance (*P*-value = 0.11033, **Table 22**).

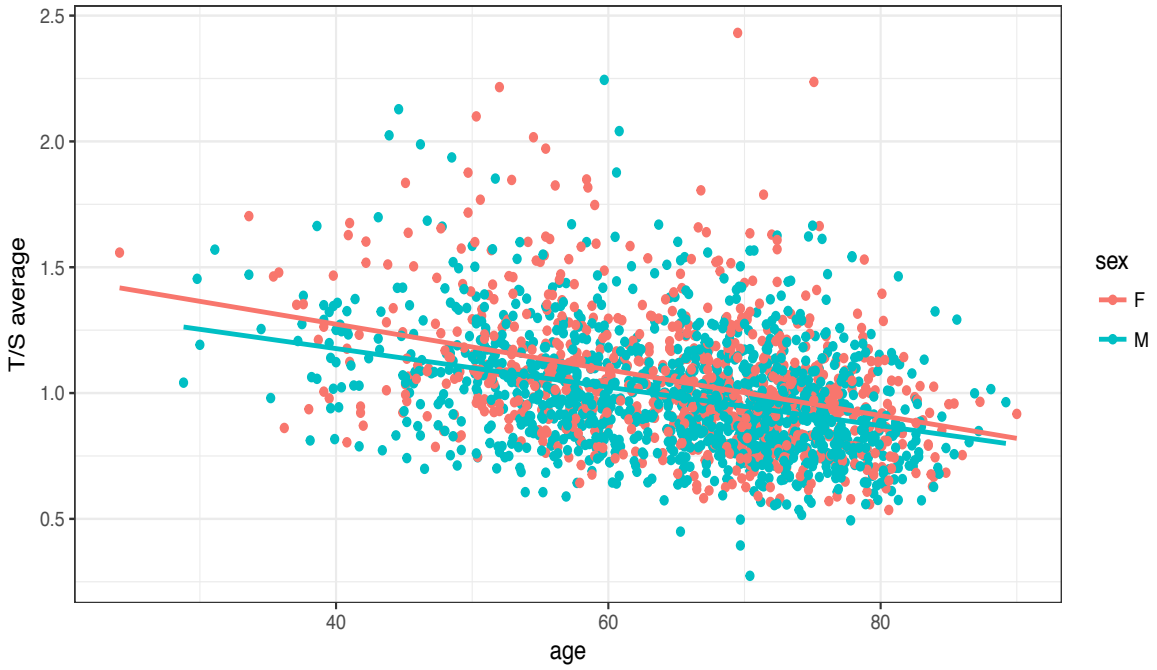

Figure 13. Association between age and relative telomere length according to sex.

In respect of smoking status, the inverse association between telomere length and age was most remarkable for subjects that were categorized as current smokers (**Figure 14)**. With increasing age, the gap between patients currently smoking and patients who had never smoked was raising. The difference in average T/S ratios between current smokers and never smokers showed statistical significance (*P*-value = 0.02613, **Table 22**). In addition, the telomere shortening in patients with former smoking habits was also found significantly different from those with no smoking history (*P*-value = 0.03998, **Table 22**).

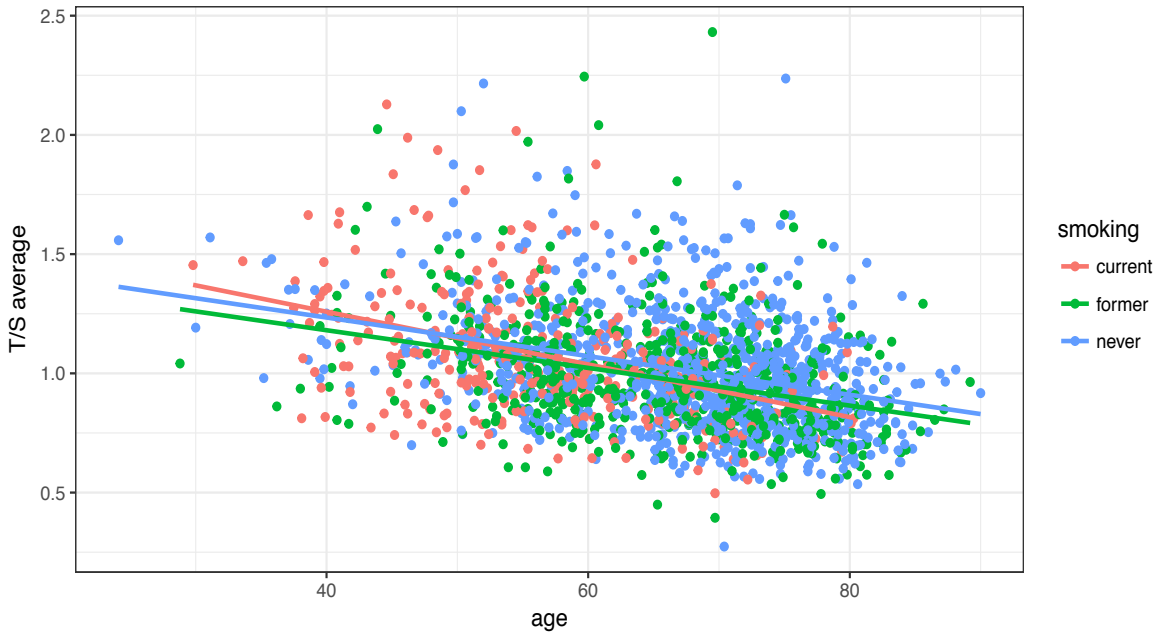

Figure 14. Association between age and relative telomere length according to smoking status.

Telomere length and histological status

Patients with colorectal carcinoma (CRC) presented a significantly longer relative telomere length than colonoscopy-negative control patients (*P*-value = 3.61×10^{-6}, **Table 22**). Relative T/S ratio in high-risk and low-risk adenoma subgroups did not significantly differ from control group (*P*-value = 0.05956 for high-risk adenomas; *P*-value = 0.05224 for low-risk adenoma subgroup, **Table 22**). In **Figure 15** the status-wise distribution of average T/S ratios of each status group is depicted as boxplots. The status effect on relative telomere length was further displayed in a bar chart (**Figure 16**). The differences of average T/S ratio compared to control group (including confidence interval) demonstrated the significant and clearly evident variation between average T/S ratio of CRC and control group.

The general distinction between young (≤ 64 years) and old (> 64 years) age group did not contribute to observe any further significant differences in average T/S ratio among patient subgroups, but resulted in decreasing statistical power (**Appendix A3, Table 24-25**).

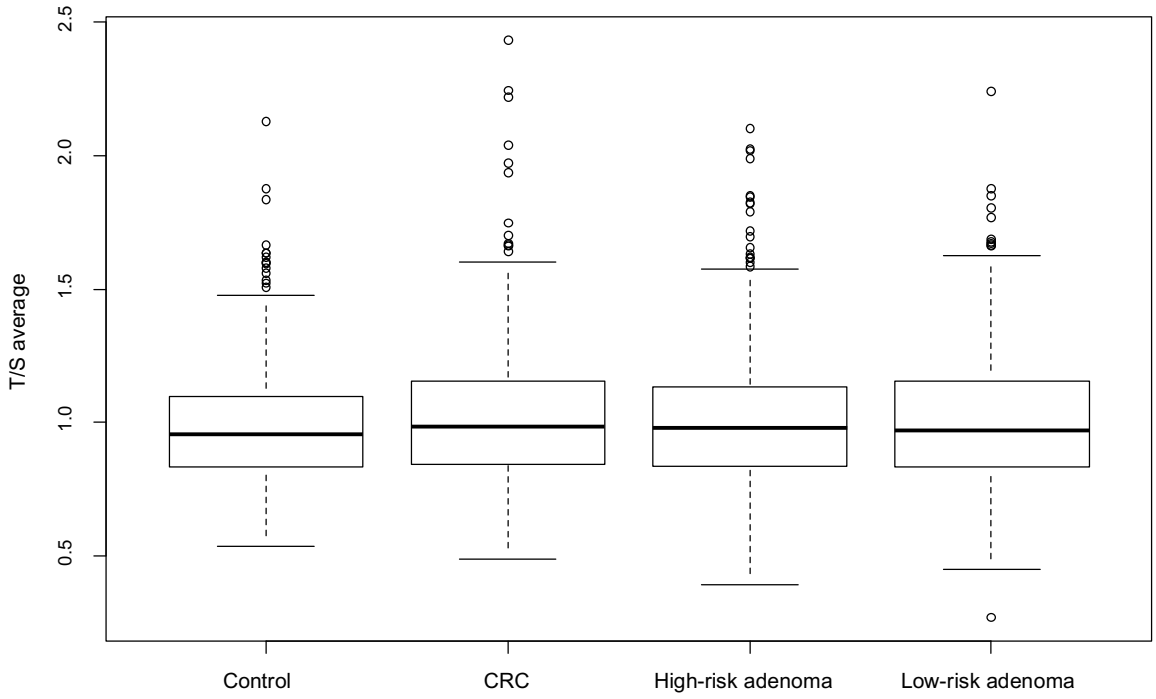

Figure 15. Status-wise distribution of average T/S ratios (derived from best multiple linear regression model).

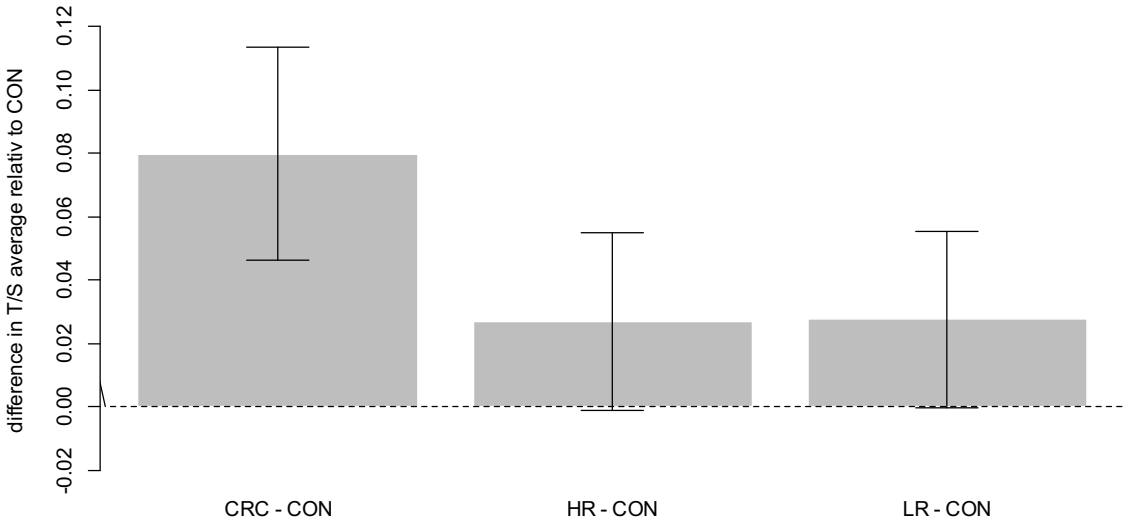

Figure 16. Status effects and confidence interval (derived from best multiple linear regression model).

5. Discussion

5.1. Functionality of MNS16A in colorectal cancer

Mutations within the TERT promoter provide the basis for reactivation of telomerase which represents a hallmark in cancer cells (Heidenreich *et al.*, 2014; Heidenreich and Kumar, 2017). Whereas mutations and VNTRs that reside within coding sequences lead to modifications of protein structure and activity, those genetic alterations when located in the 5' control region might impact on gene expression via regulation of transcription (Nakamura, Koyama and Matsushima, 1998). In this context, the functional polymorphic tandem repeat minisatellite termed MNS16A has demonstrated potential influence on expression of hTERT antisense transcript due to its concomitant location downstream of hTERT exon 16 on chromosome 5p15.33 and within the putative promoter region of antisense hTERT. Owing to its polymorphic nature, VNTR length is determined by the number of tandem repeat elements (Wang *et al.*, 2003). First evidence of MNS16A functionality was provided in a non-small cell lung cancer (NSCLC) cell line, showing that this polymorphic tandem repeat minisatellite was functionally involved as a part of the promoter that regulates the expression of an antisense hTERT transcript. Previous functional experiments suggested a link between VNTR length and promoter activity, where the shorter VNTR-243 was associated with significantly higher promoter activity than the wild-type allele VNTR-302 (Wang *et al.*, 2003). However, those assumptions were based on the investigation of only those two MNS16A VNTRs, demanding for further examination of the functional role of MNS16A and its VNTRs. Previous research of our molecular epidemiology group has led to the identification of two additional MNS16A variants: VNTR-364 was discovered in our Colorectal Cancer Study of Austria (CORSA)(Hofer *et al.*, 2011), the rare variant VNTR-212 was found in our case-control study of prostate cancer (PROSA)(Hofer *et al.*, 2013).

Therefore, promoter activity of all six known VNTRs that are potentially harbored within MNS16A were analyzed in lung and prostate cancer cell lines by our group for the first time. The present work additionally investigated MNS16A promoter activity of all known VNTRs in colorectal cancer cell lines to verify a possible correlation between promoter activity and MNS16A VNTR sequence length; results have already been published in the research journal *Oncotarget* (Hofer *et al.*, 2017).

Transient transfection of experimental MNS16A variants (VNTR-212, VNTR-243, VNTR-274, VNTR-302, VNTR-333 and VNTR-364) and a Dual-Luciferase Reporter Assay were performed in order to ascertain relative promoter activity. An inverse correlation between promoter activity and number of tandem repeat elements could be determined consistent across all tested cell lines. In the colorectal cancer cell line SW480, a simple linear model was sufficient to describe increasing promoter activity with decreasing VNTR length. Yet, the longest VNTR-364 had to be excluded from statistical analysis as it did not exhibit significantly different promoter activity compared to the promoterless negative control. In a further attempt to detect potential promoter activity of VNTR-364, the inverse correlation of promoter activity and VNTR length could only be partly confirmed in another colorectal cancer cell line HCT-116, where overall promoter activity did not significantly differ from baseline except for the shortest number of repeat elements VNTR-212 and VNTR-243.
Regarding other cancer types, for prostate cancer cell line LNCaP as well as for lung cancer cell line A-427 a more complex relationship between VNTR length and promoter activity could be characterized by a linear piecewise regression model as best model fit. A significant negative trend was similarly valid for those cell lines, although an estimated theoretical breakpoint was introduced in the linear regression. The consequent generation of two slopes with a steeper slope on the right side of the breakpoint indicated a more pronounced decrease of promoter activity for longer VNTRs (Hofer *et al.*, 2017).
As MNS16A is located downstream of hTERT gene, it is supposed to impact on gene regulation by affecting hTERT expression and consequently telomerase activity. Enhanced promoter activity and therefore elevated levels of hTERT antisense transcript may exert a repressive effect on hTERT transcription as well as telomerase activity. However, *in vitro* findings of existing antisense transcript independent of hTERT expression level put the biological function of antisense hTERT mRNA again into question (Wang *et al.*, 2003).

The functional mechanism of MNS16A may be explained through present number of CAT trinucleotide insertions within the 26 bp core sequence that could function as a potential transcription factor binding site (TFBS) for GATA binding protein 1 (GATA-1). Shorter VNTR-243 with only two CAT insertions as TBSs demonstrated enhanced promoter activity in comparison to longer VNTR-302 that contains three putative TFBs. Based on these observations it could be presumed that inhibition of promoter activity with increasing MNS16A VNTR length results from an increasing number of GATA-1 TFBSs as CAT insertions and their repressive impact (Wang *et al.*, 2003). GATA-1 belongs to a transcription

factor family (including 6 members) that is involved in cellular maturation, cell cycle control and cell survival as well as tissue development (Zheng and Blobel, 2010). Impaired transcriptional expression of GATA-4 and GATA-5 via promoter hypermethylation is known to be prevalent in colorectal carcinomas (Akiyama *et al.*, 2003; Hellebrekers *et al.*, 2009).

Apart from GATA-1, several other transcription factors such as GR-alpha (glucocorticoid receptor), XBP-1 (X-box binding protein) and TFII-I (general transcription factor II-I) are predicted to have TFBSs within the tandem repeat core sequence of MNS16A. Their functional relevance and occurrence might be dependent on cancer type and respectively tissue specifity. Considering the impact of several transcription factors on MNS16A target sequence, this already indicates the complexity of promoter activity regulation and suggests multiple potential effects of interference with telomerase expression. The results of the present study including functional analysis in prostate and lung cancer cell lines highlight the importance of different VNTR length on biological functionality and justify a precise categorization of MNS16A alleles according to the LMS classification system that favors exact distinction between overall number of repeat elements and thus TFBSs. Experimental findings *in vitro* aim to display MSN16A heterogeneity, therefore cancer cell lines serve as surrogates for tumor type specifity (Hofer *et al.*, 2017).

Multiple epidemiological studies in various ethnicities and cancer entities put emphasis on MNS16A genotyping in order to reveal associations of MNS16A genotypes and cancer susceptibility (Chen *et al.*, 2013; Xia *et al.*, 2013). Initial studies in lung cancer patients identified that an increased risk for lung cancer was prevalent in the presence of longer MNS16A alleles (LL genotype) (Wang *et al.*, 2003). However, opposing results were found in a Korean case-control study where the short allele VNTR-243 was associated with a significant increase of lung cancer risk (Jin *et al.*, 2011). In our Austrian cohort (CORSA), the allele of middle length (VNTR-274) could be related to an elevated risk of colorectal cancer (Hofer *et al.*, 2011). In contrast, a potentially protective effect of VNTR-274 was revealed in our Austrian Prostate Cancer Study (PROSA) cohort, though only among Caucasian men that exceeded the age of 70 years (Hofer *et al.*, 2013).

Two meta-analyses on MNS16A were conducted in order to comprise previous data of MNS16A genotypes and associated cancer risk (Chen *et al.*, 2013; Xia *et al.*, 2013). Including studies on breast cancer, cerebral cancer and lung cancer, an overall association between MNS16A and cancer risk was observed. Short MNS16A alleles were associated with a

significantly increased cancer risk compared to middle length alleles (Xia *et al.*, 2013). Yet, cancer-type specific analysis could only verify a significant risk association in cerebral (Chen *et al.*, 2013; Xia *et al.*, 2013) and breast cancer (Xia *et al.*, 2013), but not for lung cancer risk (Chen *et al.*, 2013; Xia *et al.*, 2013). So far, no consistent association between MNS16A and cancer risk nor certain risk alleles could be validated, even though case-control studies of sufficient design and power were considered. Varying potential of MNS16A promoter activity among different tissues may have to be taken into account with respect to interpretation of genotyping studies and classification of risk alleles. Although the exact molecular contribution of MNS16A in the process of cancer formation remains unknown, still a potential interaction of antisense RNA transcript with hTERT levels is most evident. Tumor-type and tissue specifity along with VNTR length are indicating functional heterogeneity in terms of promoter activity and TFBSs. Further cancer epidemiological studies are required with emphasis on functionality of MNS16A in connection with cancer type, before MNS16A alleles may ultimately be applied for cancer-specific risk profiling.

5.2. Telomere length and colorectal cancer risk

Telomere length of tumor tissue and peripheral blood has been intensively studied in colorectal cancer as well as in other cancer entities to investigate a potential association between telomere length and malignant transformation (Svenson and Roos, 2009; Hou *et al.*, 2012; Prescott *et al.*, 2012; Baichoo and Boardman, 2014). Regarding its clinical implication, it is essential to distinguish between approaches of telomere length in cancer tissue and peripheral blood leukocytes (PBL) as those compartments might reflect a different telomere dynamic. As blood is an easily accessible surrogate tissue, epidemiological studies have predominantly determined telomere length of peripheral blood leukocytes to understand its influence on cancer etiology (Prescott *et al.*, 2012). Telomere length of leukocyte DNA may mirror telomere length in other healthy tissues and could therefore be applied as a surrogate biomarker (Butler *et al.*, 1998; Friedrich *et al.*, 2000).

In the present work, relative PBL telomere length of 2011 individuals of the Colorectal Cancer Study of Austria (CORSA) was measured. Patients with colorectal carcinoma (384), high-risk colorectal adenoma (544) and low-risk colorectal adenoma (537) as well as colonoscopy-negative controls (546) were involved. Considering independent variables (age, sex and

smoking status) in a multiple linear regression model, relative telomere length was found to be significantly longer in patients with CRC compared to colonoscopy-negative controls.
Longer telomeres at the time of cancer diagnosis that were observed in this study might be attributed to several influencing factors. The process of telomere attrition may be decelerated in cancer patients due to a possible activation of telomere elongation mechanisms in the blood close to cancer diagnosis (Gu, 2015). In the course of tumor formation, telomeres in peripheral blood leukocytes could be extended by a general activation of the immune system (Hou *et al.*, 2012). When telomeres in surrogate tissue reach a critically short length, the activity of telomerase as well as alternative lengthening mechanisms of telomeres could preserve telomere length and prevent telomere attrition (Spyridopoulos *et al.*, 2008). Relating to colorectal tissue, longer telomeres may cause delayed senescence of cells and could favor the acquisition of genomic instability, therefore present an increased risk of oncogenesis (Mooi and Peeper, 2006). Cells featuring longer telomeres might be more likely to develop stem-cell properties and so harbor cancer-initiating mutations that increase the risk for colorectal adenoma and carcinoma formation (Jones *et al.*, 2012). Longer telomeres in colorectal carcinoma tissue were linked to poor clinical prognosis and advanced tumor stages (Gertler *et al.*, 2004; Garcia-Aranda *et al.*, 2006). Furthermore, longer telomere length may facilitate the stabilization of chromosome ends which could act beneficially on the progression of the tumor (Svenson and Roos, 2009). In contrast, telomere shortening in colorectal mucosa was also associated with genomic instability and consequently leading to neoplasia (O'Sullivan *et al.*, 2006). Abnormal changes of telomere length on both extremely long or short sides favor telomere dysfunction and chromosomal instability (CIN), a process that seems to emerge at an early stage of cancer development (Meeker *et al.*, 2004).

There are numerous reasons why epidemiological studies have shown inconsistent results regarding a possible association between CRC risk and telomere length so far. A retrospective study, where blood has been collected after CRC diagnosis, has linked shorter telomere length in blood leukocytes with elevated risk for colorectal carcinoma (Pooley *et al.*, 2010). In contrast, three case-control studies with a prospective study design could not reveal any association between leukocyte telomere length and CRC risk (Zee *et al.*, 2009; Lee *et al.*, 2010; Pooley *et al.*, 2010). Those findings might be an indication that telomere attrition could mostly take place in the progression of CRC and after cancer diagnosis. In this regard, a retrospective study design could have limited significance in terms of cause or consequence of telomere alterations and a possible reverse causation problem. It still remains unclear whether changes in telomere length

in the blood result as a response during cancer progression or if leukocyte telomeres itself contribute to the onset of CRC (Svenson and Roos, 2009). The presence of a tumor could impact on the immune system, an inflammatory response mediated through reactive oxygen species (ROS) or cytokines could potentially unbalance telomere homeostasis (Hu and Insel, 1999; Akiyama *et al.*, 2002). Moreover, a mutual interaction between development of CRC and adjustments of telomeres in the blood cannot be excluded (Svenson and Roos, 2009).
Thus, the design of the study could present one of the major contributing factors responsible for controversial findings. The interval between blood sampling and cancer development and diagnosis is an essential confounding factor that has to be taken into consideration in terms of interpretation of telomere length as a biomarker for CRC risk. Temporal differences between blood collection and cancer development limit the comparison of prospective versus retrospective studies (Prescott *et al.*, 2012).

Varying proportions of leukocyte subtypes in CRC patients and colonoscopy-negative control patients might contribute to the finding of longer telomeres in the CRC subgroup (Spyridopoulos *et al.*, 2008). Telomere length was determined of a mixture of different leukocyte subpopulations, which all proportionally contribute to the general leukocyte telomere length (Aviv, Valdes and Spector, 2006). Within different subsets of leukocytes, telomere length was found to vary – for instance granulocytes are known to have longer telomeres than lymphocytes (Rufer *et al.*, 1999). Although telomere length declines in hematopoietic cells, the activity of telomerase could be detected in peripheral blood leukocytes (Broccoli, Young and de Lange, 1995). In this context, the importance of leukocyte subsets in the carcinogenesis of CRC still needs to be clarified. Furthermore, the relative PBL telomere length does not provide insight on telomere length of specific chromosomes which may also be essential for the initiation of malignant transformation (Hou *et al.*, 2012).
Additionally, the exposure to chemotherapy or radiotherapy could cause DNA damage and telomere erosion in cancer patients (Schröder *et al.*, 2001; Unryn *et al.*, 2006). To exclude this fundamental confounding effect, in this study only CRC patients were included that had not received chemo- or radiotherapy before the time of blood sampling to avoid modifications of PBL telomere length.

Further, this study confirmed the inverse correlation between PBL telomere length and age that has been previously shown in the literature (Valdes *et al.*, 2005; Aubert and Lansdorp, 2008; Willeit *et al.*, 2010; Cui *et al.*, 2012; Boardman *et al.*, 2014). However, due to various

environmental influences (Epel *et al.*, 2004; Valdes *et al.*, 2005) and genetic distinctions (Slagboom, Droog and Boomsma, 1994; Vasa-Nicotera *et al.*, 2005), telomere length in leukocytes varies remarkably between individuals among the same age (Lin, Epel and Blackburn, 2012).

Regarding sex, the results of this study demonstrated that accelerated telomere shortening with age was generally more pronounced in women. Especially for younger female subjects a higher T/S ratio was found compared to their male counterparts. However, the interaction between sex and age was not statistically significant since average telomere length of male and female subjects converged with increasing age. Age-adjusted telomere length seems to be influenced by gender, thus adult women previously already presented longer telomeres than men (Nawrot *et al.*, 2004; Willeit *et al.*, 2010; Cui *et al.*, 2012). The effect of the female hormone estrogen may be accountable for longer PBL telomere length in women (Benetos *et al.*, 2001; Mayer *et al.*, 2006): The hormone's anti-oxidative potential might support to maintain telomere homeostasis (Aviv, 2002), signaling via the estrogen receptor-alpha could also stimulate activity of telomerase (Calado *et al.*, 2009). Since estrogen levels are declining with age, this potentially protecting effect on telomeres could cease over lifetime and contribute to the converging PBL telomere length between women and men.

In terms of smoking habits, the inverse association between telomere length and age was most pronounced for subjects with current positive smoking status. Individuals currently smoking presented significantly stronger telomere shortening with age compared to those subjects that had never smoked. Therefore, the difference in average T/S ratios between current smokers and never smokers was most remarkable with increasing age. Additionally, telomere attrition in subjects with former smoking habits was also found to be significantly stronger than in those individuals with no smoking history. A correlation between smoking and shortened PBL telomere length has already been demonstrated (Nawrot *et al.*, 2004; Huzen *et al.*, 2014), with telomere attrition proportional to the number of smoked cigarettes (Valdes *et al.*, 2005; Astuti *et al.*, 2017). Free radicals are generated by cigarette smoke, inducing oxidative stress and triggering inflammation. As a result, this could cause telomere erosion and consequently telomere shortening (Asami *et al.*, 1996).

The principle of hybridization to telomere repetitive sequences represents the basis for all telomere length determination methods. Besides determinating terminal restriction fragment (TRF) length by Southern Blotting as the "golden standard" method, quantitative fluorescence in situ hybridization (Q-FISH), flow fluorescence in situ hybridization (flow-FISH) and qPCR (single- and multiplex) methods are the most commonly used techniques to determine telomere length. Application of various telomere length measurement methods and differences in sample preparation and processing like DNA extraction method (Cunningham *et al.*, 2013) may further contribute to the inconsistency in literature concerning PBL telomere alterations in cancer patients (Svenson and Roos, 2009).

In the present study, a monochrome multiplex quantitative PCR (MMQPCR) protocol was used to determine relative PBL telomere length, expressed as average T/S ratio. This method is highly reproducible, cost-effective and therefore most suitable for high-throughput in epidemiological studies (Montpetit *et al.*, 2014). It only requires a small amount of genomic DNA and due to the specific primer design the formation of primer dimers is reduced. T/S ratios of this MMQPCR were correlating with Southern Blot and the corresponding Terminal Restriction Fragment (TRF) lengths, even stronger than for the singleplex qPCR method (Cawthon, 2009). Relative PBL telomere length was yielded by normalization on two levels: Telomere copy number was related to the expression of the single copy gene albumin to compensate for different quantities of DNA used, limiting variation between measurements. To standardize between all plates, obtained average T/S ratios of samples were compared to the ratio between telomere repeats and single copy gene of the reference DNA (consisting of 30 CORSA control patients) which resulted as 1. T/S ratios ≥1 represented longer telomeres than measured for the reference DNA, whereas T/S ratios ≤1 described a telomere length shorter relatively to the reference DNA pool. Comparing results to previous research on PBL telomere length using qPCR, it is important to point out that relative telomere length measurements are dependent on the selection of the reference DNA as they refer to the specific ratio of telomere repeats to single copy gene present in this standard DNA. Regarding the general interpretation of relative PBL telomere length, it is necessary to consider the composition of the chosen standard which may restrain comparability between different studies.

The main strengths of this study are based on the large sample size and the homogenous study population. The control group was selected within the Austrian screening program B-PREDICT and had not exhibited any colorectal pathological findings. Due to patient recruitment within this screening program, sample selection of all subgroups was conducted population-based. Besides gender- and age-matched groups, this work involved patients throughout the adenoma-carcinoma sequence. Apart from CRC patients, individuals with premalignant colorectal lesions such as high-risk adenomas and low-risk adenomas were included to capture the whole spectrum of putative CRC development.

Telomere length data on peripheral blood leukocytes including the continuum of colorectal carcinogenesis has not been published in the literature so far. Regarding high-risk colorectal adenomas, one study found PBL telomere length to be shorter in patients manifesting advanced adenomas than in the colonoscopy-negative group. The authors claimed that shorter telomere length in leukocytes might be a non-invasive biomarker to identify individuals with a higher risk for colorectal neoplasia and therefore a greater demand for this group to undergo colonoscopy. However, sample sizes were considerably small, involving only 35 patients with advanced adenomas and 145 control patients. Further, this study had a retrospective design and no information was provided on the time of blood sampling in relation to the development of advanced colorectal adenomas. A high variability of relative telomere length was shown as a singleplex qPCR method was applied. The sum of these confounding factors limits the validity of those results on PBL telomere length for detection of advanced adenomas (Riegert-Johnson *et al.*, 2012).

Regarding CRC, a comparably large retrospective case-control study revealed an association between the age of CRC onset and PBL telomere length. In a study population of 580 CRC patients and 2,081 healthy controls they found that both longer telomeres in younger individuals (≤ 50 years) as well as shorter telomeres in older individuals (> 50 years) were linked to an increased risk for CRC. Despite the large sample size, this study exhibited some limitations regarding sample selection and telomere length measurement method. Sample collection occurred within a 2-year time frame of CRC diagnosis. Although they only used chemotherapy naive patient material, this heterogeneity in relation to telomere length changes prior and post cancer diagnosis might impair the interpretation of PBL telomere length and the risk for CRC. Also, the majority of the control patients were not checked for prior colorectal polyp in their medical history. Further, a singleplex qPCR method was applied that resulted in a high inter-assay variability (16%) and therefore reduced precision and

comparability (Boardman *et al.*, 2014). In the Shanghai Women's Study, telomere length in peripheral blood of 441 women with CRC and 549 matched controls was analysed in a nested case-control approach. Similarly, findings indicated an elevated risk for CRC in the presence of very short and very long PBL telomere length. Though telomere length was determined by multiplex qPCR measurements, inter-plate variation (12-16%) was notably high (Cui *et al.*, 2012).

In the present work, an equal sample collection and processing procedure guaranteed exclusion of methodological bias between subgroups. The application of the MMQPCR protocol enabled high signal data consistency and comparability throughout all measured samples. Intra-plate variation ranged ≤ 1.9% for telomere signals (T) and ≤ 0.9% for single copy gene signals (S). Accordingly, inter-plate variation was respectively low with around 5.0% for telomeric repeats and 1.9% for albumin gene.

Although this study showed a highly significant difference in relative PBL telomere length between CRC patients and gender- and aged-matched controls, the implication of PBL telomere length as clinical biomarker is still questionable. The actual difference in relative telomere length is considerably small, the interpretation for applicability in the detection or prognosis of CRC is therefore limited relating to this type of study design. In this regard, a single time measurement of PBL telomere length might not be sufficient to assess the association between colorectal adenoma and cancer risk and telomere length in peripheral blood. As a future perspective, it could be possible to determine PBL telomere length of CORSA participants with multiple time points. This could reflect longitudinal dynamic changes of PBL telomere length that cannot be detected in a single time measurement. A follow-up of PBL telomere length in this study cohort could reveal the potential of telomere length in peripheral blood as a marker for CRC and colorectal adenoma risk and outcome.

5.2.1. Conclusion

Telomere length of surrogate tissue such as peripheral blood leukocytes could be a potential and powerful tool to assess the risk of CRC. However, there are several confounders that might restrain the interpretation of the complex association between PBL telomere length and CRC development. To enhance the understanding of cancer initiation and its link to telomere length in the blood, epidemiological telomere research has to consider multiple telomere dynamics. Since the inter-individual variation of telomere length is reasonably high among patients at the same age, this already indicates the difficulty of establishing a 'normal range' of PBL telomere length that could be applied as a clinical biomarker in CRC malignancy.

Yet, PBL telomere length remains a field of interest with the potential to contribute to early detection of CRC. In order to clarify the dynamics of PBL telomere length in the initiation and progression of CRC, large longitudinal studies could support its evaluation and its suitability as biomarker for CRC.

Appendix

A1. Vector maps

Vectors that were used for transfection experiments of colorectal cancer cell lines are displayed in **Figure 17-26**.

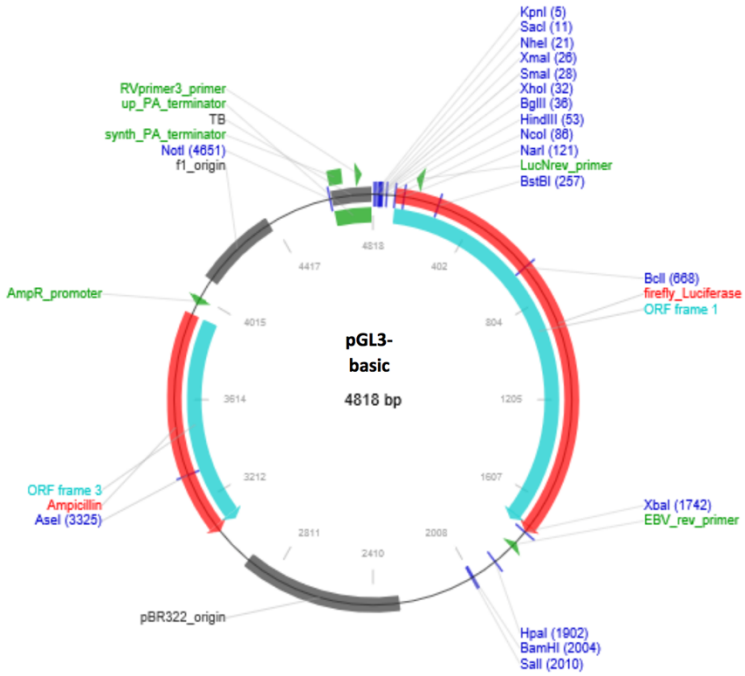

Figure 17. pGL3-basic vector map (Addgene, 2017).

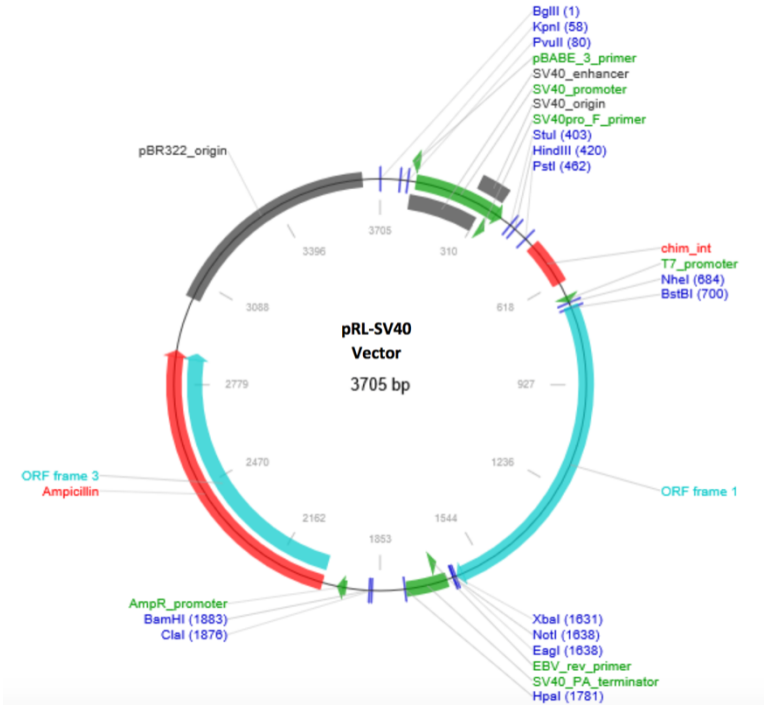

Figure 18. pRL-SV40 vector map (Addgene, 2017).

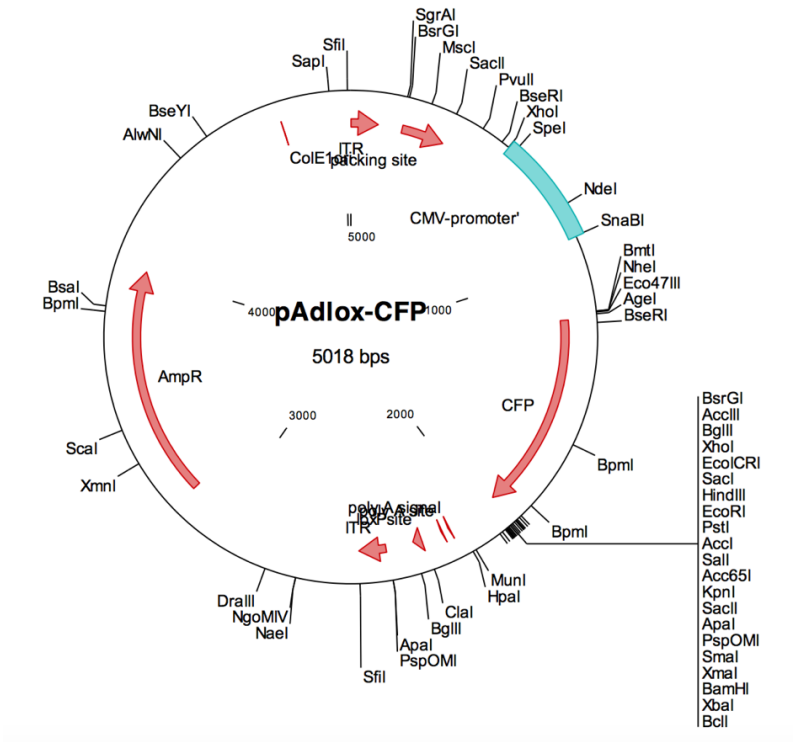

Figure 19. pAdlox CFP vector map.

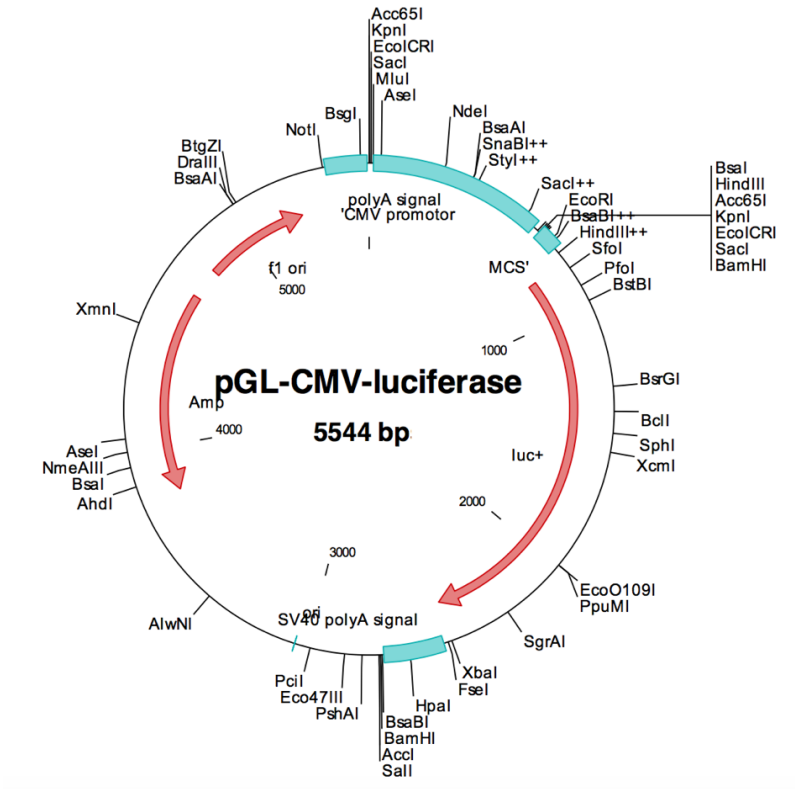

Figure 20. pGL CMV luciferase vector map.

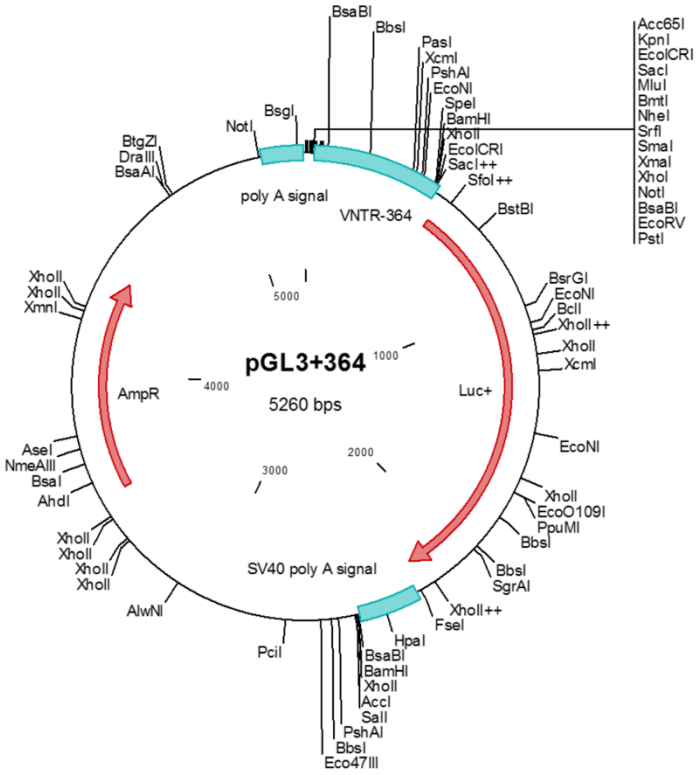

Figure 21. pGL3_MNS16A VNTR-364 vector map.

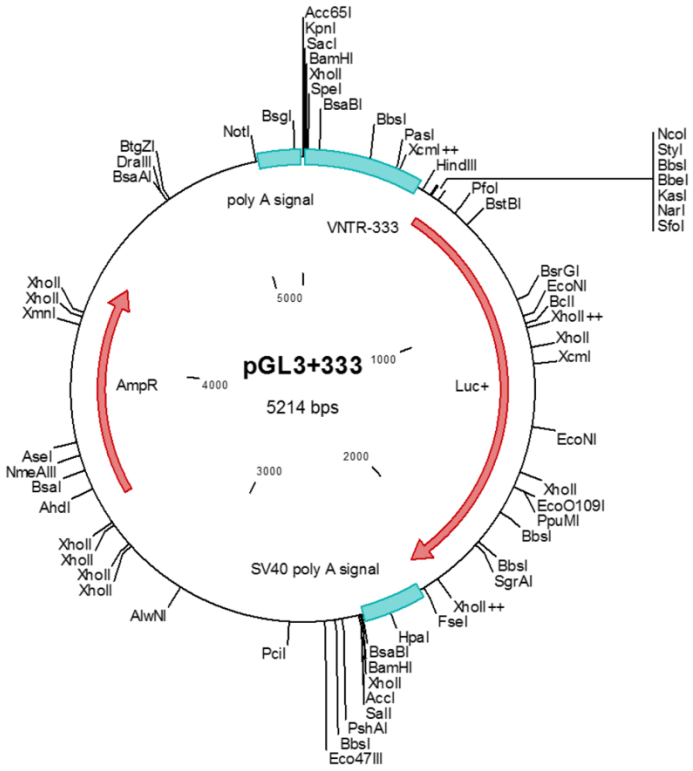

Figure 22. pGL3_MNS16A VNTR-333 vector map.

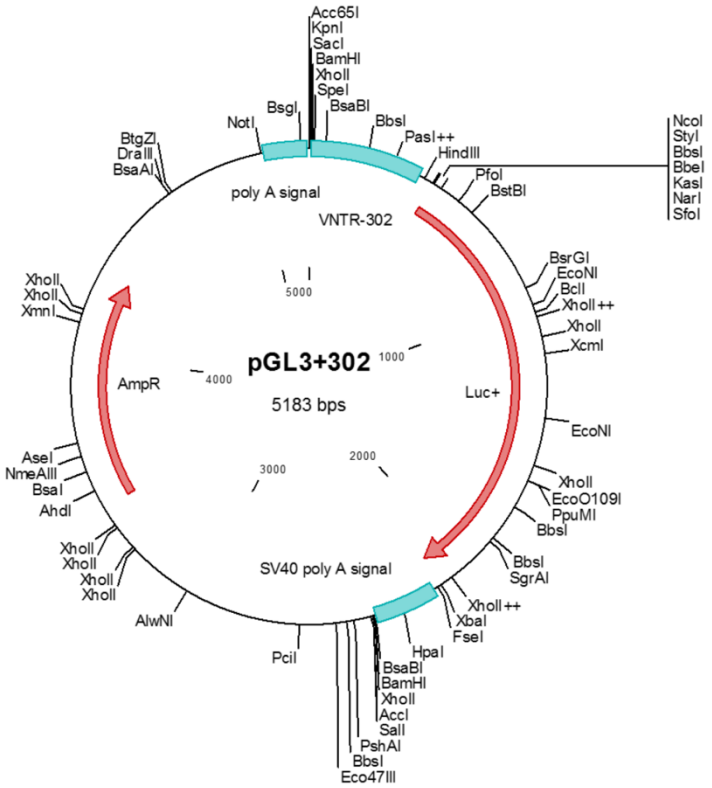

Figure 23. pGL3_MNS16A VNTR-302 vector map.

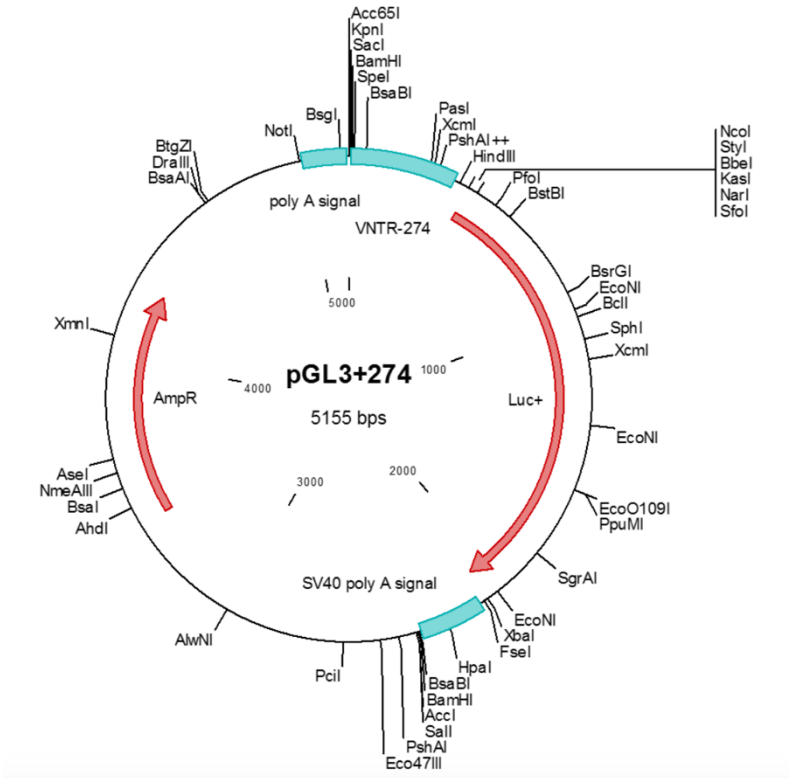

Figure 24. pGL3_MNS16A VNTR-274 vector map.

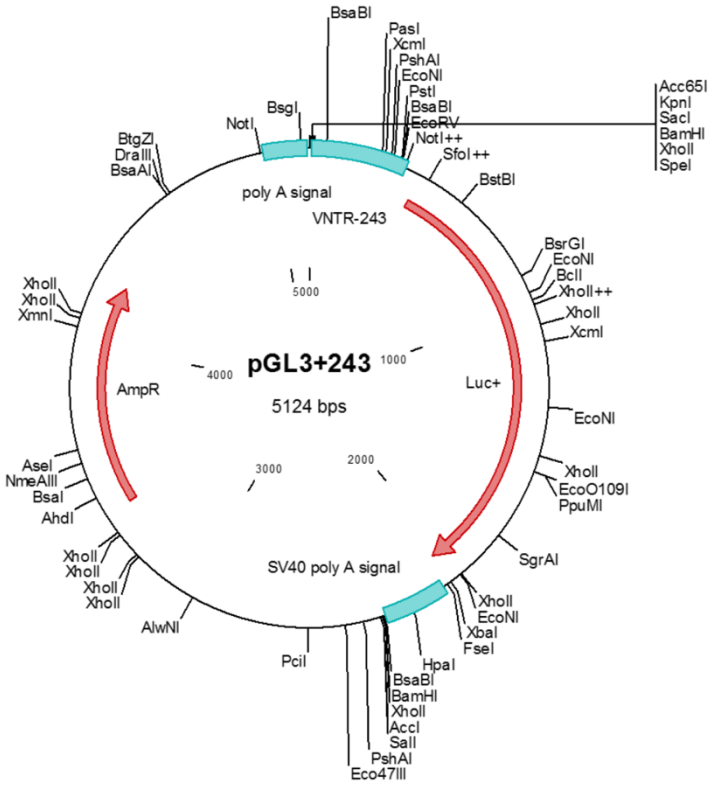

Figure 25. pGL3_MNS16A VNTR-243 vector map.

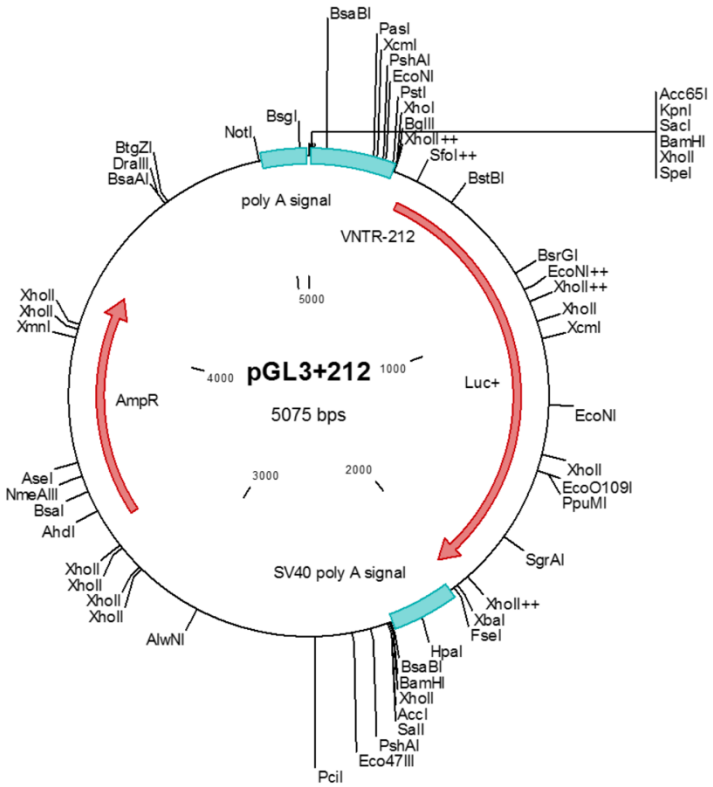

Figure 26. pGL3_MNS16A VNTR-212 vector map.

A2. Inter-plate variation of relative telomere length measurement

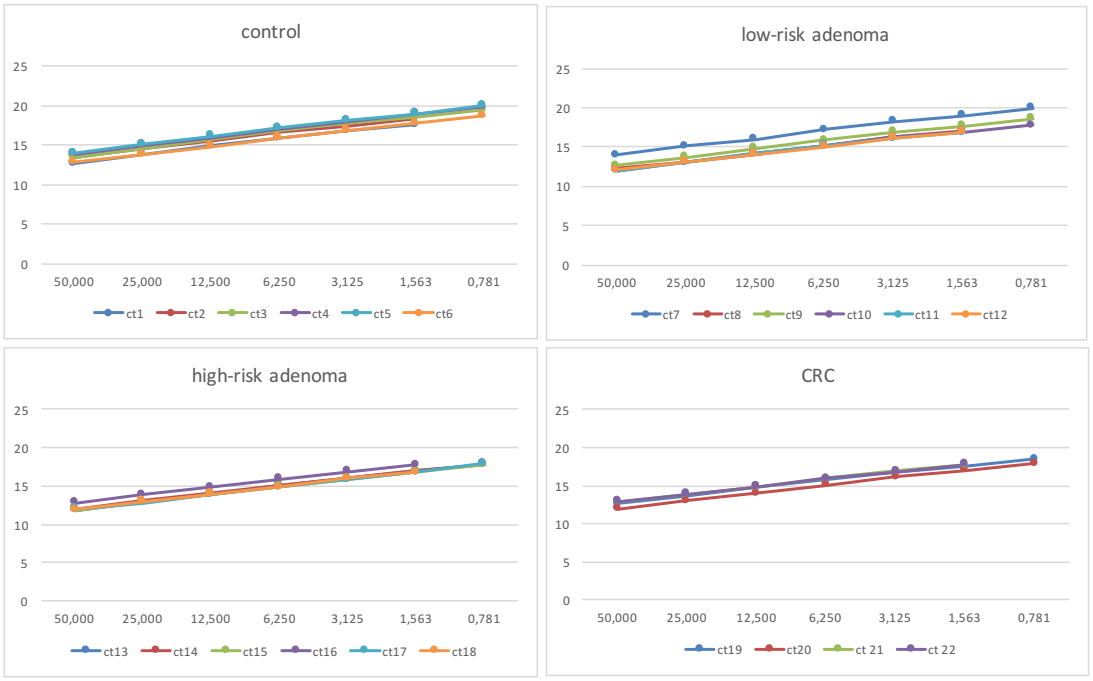

Figure 27. Inter-plate variation for telomere repeats (T): Standard straight line of each run, Ct values on y-axis versus amount of DNA [ng] on x-axis.

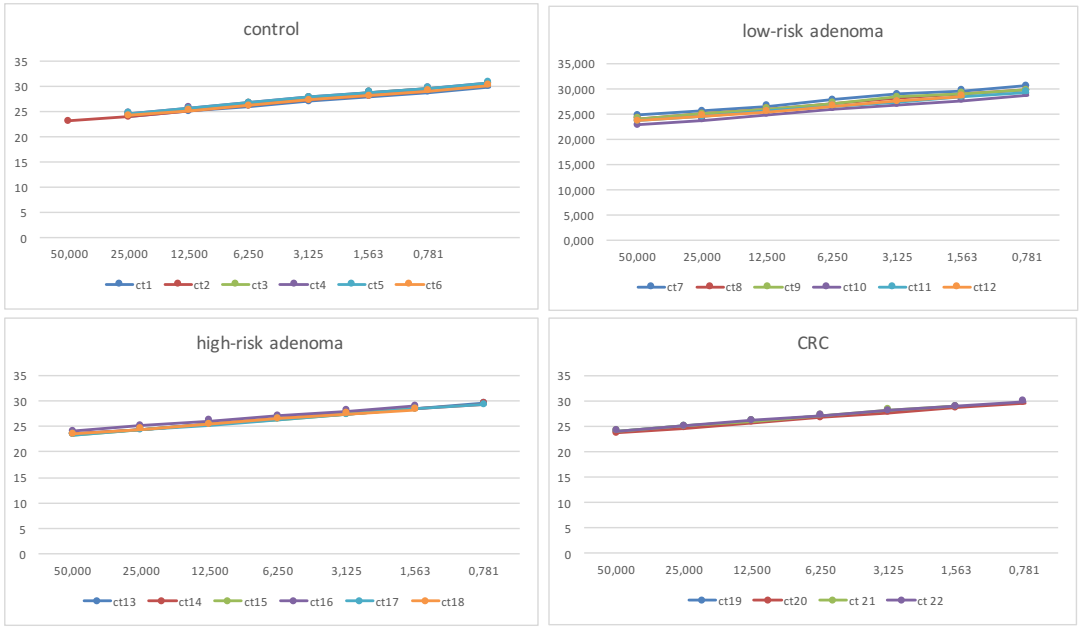

Figure 28. Inter-plate variation for single gene (albumin) signals (S): Standard straight line of each run, Ct values on y-axis versus amount of DNA [ng] on x-axis.

A3. Regression models of relative telomere length

Table 23. Effect of status, age, sex, smoking and interactions with age on relative telomere length

Model: status + age, sex, smoking + interactions with age (163 with smoking missing excluded)				
	Estimate	**Std. Error**	**t value**	**Pr(>|t|)**
(Intercept)	0.9809600	0.0212337	46.198	< 2e-16 ***
Age	-0.0118636	0.0017319	-6.850	1.01e-11 ***
Sex Male	-0.0521191	0.0117988	-4.417	1.06e-05 ***
status CRC	0.0799569	0.0172258	4.642	3.70e-06 ***
status HR	0.0267898	0.0142818	1.876	0.06084 .
status LR	0.0276598	0.0142177	1.945	0.05187 .
Former smoker	0.0159815	0.0193777	0.825	0.40963
Never smoker	0.0484969	0.0187374	2.588	0.00972 **
Age:sex Male	0.0017404	0.0010964	1.587	0.11261
Age:status CRC	-0.0007501	0.0015517	-0.483	0.62886
Age:status HR	-0.0013267	0.0013410	-0.989	0.32262
Age:status LR	-0.0002508	0.0013399	-0.187	0.85156
Age:Former smoker	0.0032576	0.0016080	2.026	0.04292 *
Age:Never smoker	0.0032624	0.0015247	2.140	0.03252 *

Table 24. Effect of status and combined effect of status, age, sex and smoking on relative telomere length among patients up to the age of 64 years

Model: status only, age ≤ 64				
	Estimate	**Std. Error**	**t value**	**Pr(>|t|)**
(Intercept)	1.06753	0.01755	60.840	<2e-16 ***
status CRC	0.05254	0.02741	1.917	0.0556 .
status HR	0.03855	0.02496	1.545	0.1228
status LR	0.03120	0.02493	1.251	0.2111
Model: status + age, sex, smoking (97 with smoking missing excluded)				
	Estimate	**Std. Error**	**t value**	**Pr(>|t|)**
(Intercept)	1.593267	0.077166	20.647	< 2e-16 ***
Age	-0.008732	0.001396	-6.255	6.78e-10 ***
Sex Male	-0.069919	0.019434	-3.598	0.000343 ***
status CRC	0.094797	0.030405	3.118	0.001894 **
status HR	0.036737	0.024502	1.499	0.134219
status LR	0.034151	0.024294	1.406	0.160231
Former smoker	-0.041283	0.023752	-1.738	0.082626 .
Never smoker	0.006316	0.023227	0.272	0.785750

Table 25. Effect of status and combined effect of status, age, sex and smoking on relative telomere length among patients above the age of 64 years

Model: status only, age > 64				
	Estimate	**Std. Error**	**t value**	**Pr(>|t|)**
(Intercept)	0.93598	0.01220	76.720	<2e-16 ***
status CRC	0.03340	0.01898	1.760	0.0787 .
status HR	0.01148	0.01727	0.665	0.5064
status LR	0.01841	0.01736	1.060	0.2893
Model: status + age, sex, smoking (97 with smoking missing excluded)				
	Estimate	**Std. Error**	**t value**	**Pr(>|t|)**
(Intercept)	1.542946	0.092040	16.764	< 2e-16 ***
Age	-0.009008	0.001264	-7.129	1.83e-12 ***
Sex Male	-0.043251	0.014682	-2.946	0.003288 **
status CRC	0.070316	0.020435	3.441	0.000601 ***
status HR	0.018781	0.017305	1.085	0.278039
status LR	0.023005	0.017284	1.331	0.183469
Former smoker	0.056215	0.026310	2.137	0.032845 *
Never smoker	0.077351	0.025274	3.060	0.002263 **

References

Ã, J. W. S. and Wright, W. E. (2005) 'Senescence and immortalization: role of telomeres and telomerase', *Carcinogenesis*, 26(5), pp. 867–874.

Addgene (2017) *The nonprofit plasmid repository*, availabe from: *https://www.addgene.org/vector-database/*.

Akincilar, S. C., Unal, B. and Tergaonkar, V. (2016) 'Reactivation of telomerase in cancer', *Cellular and Molecular Life Sciences*, 73(8), pp. 1659–1670.

Akiyama, M. *et al.* (2002) 'Cytokines modulate telomerase activity in a human multiple myeloma cell line', *Cancer Research*, 62(13), pp. 3876–3882.

Akiyama, Y. *et al.* (2003) 'GATA-4 and GATA-5 Transcription Factor Genes and Potential Downstream Antitumor Target Genes Are Epigenetically Silenced in Colorectal and Gastric Cancer', *Molecular and Cellular Biology*, 23(23), pp. 8429–8439.

Asami, S. *et al.* (1996) 'Increase of a type of oxidative DNA damage, 8-hydroxyguanine, and its repair activity in human leukocytes by cigarette smoking', *Cancer Research*, 56(11), pp. 2546–2549.

Astuti, Y. *et al.* (2017) 'Cigarette smoking and telomere length : A systematic review of 84 studies and meta-analysis', *Environmental Research*, 158, pp. 480–489.

Aubert, G. and Lansdorp, P. M. (2008) 'Telomeres and Aging', *Physiological Reviews*, 88(2), pp. 557–579.

Aviv, A. (2002) 'Telomeres, sex, reactive oxygen species, and human cardiovascular aging', *Journal of Molecular Medicine*, 80(11), pp. 689–695.

Aviv, A., Valdes, A. M. and Spector, T. D. (2006) 'Human telomere biology: Pitfalls of moving from the laboratory to epidemiology', *International Journal of Epidemiology*, 35(6), pp. 1424–1429.

Baichoo, E. and Boardman, L. A. (2014) 'Toward a Molecular Classification of Colorectal Cancer: The Role of Telomere Length', *Frontiers in Oncology*, 4:158.

Baird, D. M. (2010) 'Variation at the TERT locus and predisposition for cancer', *Expert Reviews in Molecular Medicine*, 12, p. e16.

Barker, N. *et al.* (2009) 'Crypt stem cells as the cells-of-origin of intestinal cancer', *Nature*, 457(7229), pp. 608–611.

Benetos, A. *et al.* (2001) 'Telomere length as an indicator of biological aging: the gender effect and relation with pulse pressure and pulse wave velocity.', *Hypertension*, 37(2), pp. 381–385.

Bertorelle, R. *et al.* (2014) 'Telomeres , telomerase and colorectal cancer', *World Journal of Gastroenterology*, 20(8), pp. 1940–1950.

Bisoffi, M., Heaphy, C. M. and Griffith, J. K. (2006) 'Telomeres : Prognostic markers for solid tumors', *International Journal of Cancer*, 119, pp. 2255–2260.

Blackburn, E. H. (1992) 'Telomerases', *Annual Review of Biochemistry*, 61(1), pp. 113–129.

Blackburn, E. H. and Szostak, J. W. (1984) 'The Molecular Structure of Centromeres and Telomeres', *Annual Review of Biochemistry*, 53(1), pp. 163–194.

Boardman, L. A. *et al.* (2014) 'The Association of Telomere Length with Colorectal Cancer Differs by the Age of Cancer Onset', *Clinical and Translational Gastroenterology*, 5, pp. e52-8.

Brabletz, T. *et al.* (2005) 'Migrating cancer stem cells - an integrated concept of malignant tumour progression', *Nature Reviews Cancer*, 5(9), pp. 744–749.

Bresalier RS. (2002) 'Malignant neoplasms of the large intestine. In: Feldman M, Friedman LS, Sleisenger MH, editors. Sleisenger & Fordtran's gastrointestinal and liver disease: pathophysiology, diagnosis, management.', in *7th ed. Philadelphia: Saunders*, pp. 2215–2261.

Broccoli, D., Young, J. W. and de Lange, T. (1995) 'Telomerase activity in normal and malignant hematopoietic cells', *Proceedings of the National Academy of Sciences of the United States of America*, 92(20), pp. 9082–9086.

Butler, M. G. *et al.* (1998) 'Comparison of Chromosome Telomere Integrity in Multiple Tissues from Subjects at Different Ages', *Cancer Genetics and Cytogenetics*, 105(2), pp. 138–144.

Calado, R. T. *et al.* (2009) 'Sex hormones , acting on the TERT gene , increase telomerase activity in human primary hematopoietic cells', *Hematopoiesis and stem cells*, 114, pp. 2236–2244.

Carpentier, C. *et al.* (2007) 'Association of telomerase gene hTERT polymorphism and malignant gliomas', *Journal of Neuro-Oncology*, 84(3), pp. 249–253.

Cawthon, R. M. (2009) 'Telomere length measurement by a novel monochrome multiplex quantitative PCR method', *Nucleic Acids Research*, 37(3), pp. 1–7.

Chen, C.-H. and Chen, R.-J. (2011) 'Prevalence of Telomerase Activity in Human Cancer', *Journal of the Formosan Medical Association*, 110(5), pp. 275–289.

Chen, P. *et al.* (2013) 'The TERT MNS16A polymorphism contributes to cancer susceptibility: Meta-analysis of the current studies', *Gene*, 519(2), pp. 266–270.

Chen, Y. *et al.* (2014) 'Short leukocyte telomere length predicts poor prognosis and indicates altered immune functions in colorectal cancer patients', *Annals of Oncology*, 25(4), pp. 869–876.

Collins, K. and Mitchell, J. R. (2002) 'Telomerase in the human organism', *Oncogene*, 21, pp. 564–579.

Colucci, P. M., Yale, S. H. and Rall, C. J. (2003) 'Colorectal Polyps', *Clinical Medicine and Research*, 1(3), pp. 261–262.

Counter, C. M. *et al.* (1992) 'Telomere shortening associated with chromosome instability is arrested in immortal cells which express telomerase activity', *The EMBO Journal*, 11(5), pp. 1921–1929.

Counter, C. M. *et al.* (1998) 'Telomerase activity is restored in human cells by ectopic expression of hTERT (hEST2), the catalytic subunit of telomerase', *Oncogene*, 16, pp. 1217–1222.

Cui, Y. *et al.* (2012) 'Association of leukocyte telomere length with colorectal cancer risk: nested case-control findings from the Shanghai Women's Health Study', *Cancer epidemiology, biomarkers and prevention*, 21(10), pp. 1807–1813.

Cunningham, J. M. *et al.* (2013) 'Telomere Length Varies By DNA Extraction Method: Implications for Epidemiologic Research', *Cancer Epidemiol. Biomarkers and Prevention*, 22(11), pp. 2047–2054.

Engelhardt, M. *et al.* (1997) 'Telomerase and telomere length in the development and progression of premalignant lesions to colorectal cancer', *Clinical Cancer Research*, 3(11), pp. 1931–1941.

Epel, E. S. *et al.* (2004) 'Accelerated telomere shortening in response to life stress', *Proceedings of the National Academy of Sciences*, 101(49), pp. 17312–17315.

Erichsen, R. *et al.* (2016) 'Increased Risk of Colorectal Cancer Development Among Patients With Serrated Polyps', *Gastroenterology*, 150(4), p. 895–902.e5.

Feng, J. *et al.* (1995) 'The RNA component of human telomerase', *Science*, 269(5228), pp. 1236–1241.

Ferlay, J. *et al.* (2013) 'Cancer incidence and mortality worldwide : Sources, methods and major patterns in GLOBOCAN 2012', *International Journal of Cancer*, 132(5), pp. 1133–45.

Fleming, M. *et al.* (2012) 'Colorectal carcinoma: Pathologic aspects', *Journal of Gastrointestinal Oncology*, 3(3), pp. 153–173.

Friedrich, U. *et al.* (2000) 'Telomere length in different tissues of elderly patients', *Mechanisms of Ageing and Development*, 119(3), pp. 89–99.

Garcia-Aranda, C. *et al.* (2006) 'Correlations of telomere length, telomerase activity, and telomeric-repeat binding factor 1 expression in colorectal carcinoma.', *Cancer*, 106(3), pp. 541–551.

Gertler, R. *et al.* (2004) 'Telomere length and human telomerase reverse transcriptase expression as markers for progression and prognosis of colorectal carcinoma', *Journal of Clinical Oncology*, 22(10), pp. 1807–1814.

Ghosh, A. *et al.* (2012) 'Telomerase directly regulates NF-κB-dependent transcription', *Nature Cell Biology*, 14(12), pp. 1270–1281.

Greider, C. W. and Blackburn, E. H. (1985) 'Identification of a Specific Telomere Terminal Transferase Activity in Tetrahymena Extracts', *Cell*, 43, pp. 405–413.

Greider, C. W. and Blackburn, E. H. (1996) 'Telomeres, Telomerase and Cancer', *Scientific American*, 274(2), pp. 92–97.

Griffith, J. D. *et al.* (1999) 'Mammalian Telomeres End in a Large Duplex Loop', *Cell*, 97, pp. 503–514.

Gu, J. (2015) 'Leukocyte Telomere Length and Cancer Risk: A Dynamic Problem', *EBioMedicine*, 2(6), pp. 493–494.

Hamilton, S., Bosman FT and Boffetta, P. (2010) 'Carcinoma of the colon and rectum. In: WHO Classification of Tumours of the Digestive System. Bosman FT, Carneiro F, Hruban RH, Theise ND, eds. Lyon: IARC Press', pp. 134–46.

Hanahan, D. and Weinberg, R. A. (2011) 'Review Hallmarks of Cancer : The Next Generation', *Cell*, 144(5), pp. 646–674.

Hastie, N. D. *et al.* (1990) 'Telomere reduction in human colorectal carcinoma and with ageing', *Nature*, 346(6287), pp. 866–868.

Heidenreich, B. *et al.* (2014) 'TERT promoter mutations in cancer development', *Current Opinion in Genetics & Development*, 24, pp. 30–37.

Heidenreich, B. and Kumar, R. (2017) 'TERT promoter mutations in telomere biology', *Mutation Research/Reviews in Mutation Research*, 771, pp. 15–31.

Hellebrekers, D. M. E. I. *et al.* (2009) 'GATA4 and GATA5 are Potential Tumor Suppressors and Biomarkers in Colorectal Cancer', *Clinical Cancer Research*, 15(12), pp. 3990–3997.

Hofer, P. *et al.* (2011) 'MNS16A tandem repeats minisatellite of human telomerase gene: A risk factor for colorectal cancer', *Carcinogenesis*, 32(6), pp. 866–871.

Hofer, P. *et al.* (2012) 'Association of genetic variants of human telomerase with colorectal polyps and colorectal cancer risk', *Molecular Carcinogenesis*, pp. E176–182.

Hofer, P. *et al.* (2013) 'MNS16A tandem repeat minisatellite of human telomerase gene and prostate cancer susceptibility', *Mutagenesis*, 28(3), pp. 301–306.

Hofer, P. *et al.* (2017) 'MNS16A tandem repeat minisatellite of human telomerase gene: functional studies in colorectal, lung and prostate cancer', *Oncotarget*, 8(17), pp. 28021–28027.

Hou, L. *et al.* (2012) 'Surrogate tissue telomere length and cancer risk: Shorter or Longer?', *Cancer Letters*, 319(2), pp. 130–135.

Hu, B. T. and Insel, R. A. (1999) 'Up-regulation of telomerase in human B lymphocytes occurs independently of cellular proliferation and with expression of the telomerase catalytic subunit', *European Journal of Immunology*, 29(11), pp. 3745–3753.

Huels, D. J. and Sansom, O. J. (2015) 'Stem vs non-stem cell origin of colorectal cancer', *British Journal of Cancer*, 113(1), pp. 1–5.

Huzen, J. *et al.* (2014) 'Telomere length loss due to smoking and metabolic traits', *Journal of Internal Medicine*, 275(2), pp. 155–163.

Iacopetta, B. (2003) 'TP53 mutation in colorectal cancer', *Human Mutation*, 21(3), pp. 271–276.

Jannuzzi, A. T. *et al.* (2015) 'Telomerase reverse transcriptase (TERT) gene variations and susceptibility of colorectal cancer', *Genetic Testing and Molecular Biomarkers*, 19(12), pp. 692–697.

Jin, G. *et al.* (2011) 'Dual roles of a variable number of tandem repeat polymorphism in the TERT gene in lung cancer', *Cancer Science*, 102(1), pp. 144–149.

Jones, a. M. *et al.* (2012) 'TERC polymorphisms are associated both with susceptibility to colorectal cancer and with longer telomeres', *Gut*, 61(2), pp. 248–254.

Katayama, S. *et al.* (1999) 'Clinical Usefulness of Telomerase Activity and Telomere Length in the Preoperative Diagnosis of Gastric and Colorectal Cancer', *Journal of Cancer Research and Clinical Oncology*, 125(7), pp. 405–410.

Kim, N. W. *et al.* (1994) 'Specific association of human telomerase activity with immortal cells and cancer', *Science*, 266(5193), pp. 2011–2015.

Kinnersley, B. *et al.* (2012) 'The TERT variant rs2736100 is associated with colorectal cancer risk', *British Journal of Cancer*, 107(6), pp. 1001–1008.

Lee, I.-M. *et al.* (2010) 'Mean leukocyte telomere length and risk of incident colorectal carcinoma in women: a prospective, nested case-control study', *Clinical chemistry and laboratory medicine*, 48(2), pp. 259–62.

Lengauer, C., Kinzler, K. W. and Vogelstein, B. (1998) 'Genetic instabilities in human cancers', *Nature*, 396(6712), pp. 643–649.

Leslie, A., Carey, F. and Steele, R. J. C. (2002) 'The colorectal adenoma ± carcinoma sequence', *British Journal of Surgery*, 89(7), pp. 845–860.

Lin, J., Epel, E. and Blackburn, E. (2012) 'Telomeres and lifestyle factors: Roles in cellular aging', *Mutation Research/Fundamental and Molecular Mechanisms of Mutagenesis*, 730(1–2), pp. 85–89.

Markowitz, S. D. and Bertagnolli, M. M. (2009) 'Molecular Basis of Colorectal Cancer', *New England Journal of Medicine*, 361(25), pp. 2449–2460.

Mayer, S. *et al.* (2006) 'Sex-specific telomere length profiles and age-dependent erosion dynamics of individual chromosome arms in humans', *Cytogenetic and Genome Research*, 112(3–4), pp. 194–201.

Meeker, A. K. *et al.* (2004) 'Telomere Length Abnormalities Occur Early in the Initiation of Epithelial Carcinogenesis', *Clinical Cancer Research*, 10(10), pp. 3317–3326.

Montpetit, A. J. *et al.* (2014) 'Telomere Length: A Review of Methods for Measurement', *Nursing research*, 63(4), pp. 289–299.

Mooi, W. J. and Peeper, D. S. (2006) 'Oncogene-Induced Cell Senescence — Halting on the Road to Cancer', *New England Journal of Medicine*, 355(10), pp. 1037–1046.

Morkel, M. *et al.* (2015) 'Similar but different: distinct roles for KRAS and BRAF oncogenes in colorectal cancer development and therapy resistance', *Oncotarget*, 6(25), pp. 20785–20800.

Moyzis, R. K. *et al.* (1988) 'A highly conserved repetitive DNA sequence, (TTAGGG)n, present at the telomeres of human chromosomes', *Proceedings of the National Academy of Sciences of the United States of America*, 85, pp. 6622–6626.

Naing, C. *et al.* (2017) 'Association between telomere length and the risk of colorectal cancer: a meta-analysis of observational studies', *BMC Cancer*, 17(1), p. 24.

Nakamura, T. M. and Cech, T. R. (1998) 'Reversing Time: Origin of Telomerase', *Cell*, 92(5), pp. 587–590.

Nakamura, Y., Koyama, K. and Matsushima, M. (1998) 'VNTR (variable number of tandem repeat) sequences as transcriptional, translational, or functional regulators', *Journal of Human Genetics*, 43(3), pp. 149–152.

Nawrot, T. S. *et al.* (2004) 'Telomere length and possible link to X chromosome', *The Lancet*, 363(9408), pp. 507–510.

Niiyama, H. *et al.* (2001) 'Quantitative analysis of hTERT mRNA expression in colorectal cancer', *The American Journal of Gastroenterology*, 96(6), pp. 1895–1900.

O'Sullivan, J. *et al.* (2006) 'Telomere length in the colon declines with age: A relation to colorectal cancer?', *Cancer Epidemiology Biomarkers and Prevention*, 15(3), pp. 573–577.

Palm, W. and de Lange, T. (2008) 'How Shelterin Protects Mammalian Telomeres', *Annual Review of Genetics*, 42(1), pp. 301–334.

Park, J.-I. *et al.* (2009) 'Telomerase modulates Wnt signalling by association with target gene chromatin', *Nature*, 460(7251), pp. 66–72.

Pellatt, A. J. *et al.* (2013) 'TERT's role in colorectal carcinogenesis', *Molecular Carcinogenesis*, 52(7), pp. 507–513.

Perrault, S. D., Hornsby, P. J. and Betts, D. H. (2005) 'Global gene expression response to telomerase in bovine adrenocortical cells', *Biochemical and Biophysical Research Communications*, 335(3), pp. 925–936.

Pino, M. S. and Chung, D. C. (2010) 'The chromosomal instability pathway in colon cancer', *Gastroenterology*, 138(6), pp. 2059–2072.

Pooley, K. A. *et al.* (2010) 'Telomere length in prospective and retrospective cancer case-control studies', *Cancer Research*, 70(8), pp. 3170–3176.

Prescott, J. *et al.* (2012) 'Epidemiologic evidence for a role of telomere dysfunction in cancer etiology', *Mutation Research - Fundamental and Molecular Mechanisms of Mutagenesis*, 730(1–2), pp. 75–84.

Preston, S. L. *et al.* (2003) 'Bottom-up histogenesis of colorectal adenomas: Origin in the monocryptal adenoma and initial expansion by crypt fission', *Cancer Research*, 63(13), pp. 3819–3825.

Pucci, F., Gardano, L. and Harrington, L. (2013) 'Short telomeres in ESCs lead to unstable differentiation', *Cell Stem Cell*, 12(4), pp. 479–486.

Qi, H. *et al.* (2012) 'TERT rs2736098 polymorphism and cancer risk : results of a meta-analysis', *Asian Pacific Journal of Cancer Prevention*, 13, pp. 3483–3488.

Qin, Q. *et al.* (2014) 'Telomere length in peripheral blood leukocytes is associated with risk of colorectal cancer in Chinese population', *PLoS ONE*, 9(2), p. e88135.

R Core Team (2017) 'R: A language and environment for statistical computing.'

Rajagopalan, H. *et al.* (2002) 'Tumorigenesis: RAF/RAS oncogenes and mismatch-repair status', *Nature*, 418(6901), p. 934.

Rampazzo, E. *et al.* (2010) 'Relationship between telomere shortening , genetic instability, and site of tumour origin in colorectal cancers', *British Journal of Cancer*, 102(8), pp. 1300–1305.

Raynaud, C. M. *et al.* (2008) 'Telomere shortening is correlated with the DNA damage response and telomeric protein down-regulation in colorectal preneoplastic lesions', *Annals of Oncology*, 19, pp. 1875–1881.

Riegert-Johnson, D. L. *et al.* (2012) 'Shorter peripheral blood telomeres are a potential biomarker for patients with advanced colorectal adenomas', *The International Journal of Biological Markers*, 27(4), pp. e375-80.

Rufer, N. *et al.* (1999) 'Telomere Fluorescence Measurements in Granulocytes and T Lymphocyte Subsets Point to a High Turnover of Hematopoietic Stem Cells and Memory T Cells in Early Childhood', *The Journal of Experimental Medicine*, 190(2), pp. 157–167.

Sangiorgi, E. and Capecchi, M. R. (2008) 'Bmi1 is expressed in vivo in intestinal stem cells', *Nature Genetics*, 40(7), pp. 915–920.

Sansom, O. J. *et al.* (2004) 'Loss of Apc in vivo immediately perturbs Wnt signaling, differentiation, and migration', *Genes and Development*, 18(12), pp. 1385–1390.

Schröder, C. P. *et al.* (2001) 'Telomere length in breast cancer patients before and after chemotherapy with or without stem cell transplantation', *British Journal of Cancer*, 84(10), pp. 1348–1353.

Schwitalla, S. *et al.* (2013) 'Intestinal tumorigenesis initiated by dedifferentiation and acquisition of stem-cell-like properties', *Cell*, 152(1–2), pp. 25–38.

Sharpless, N. E. and Depinho, R. A. (2004) 'Telomeres, stem cells, senescence, and cancer', *The Journal of Clinical Investigation*, 113(2), pp. 160–168.

Shay, J. W. and Bacchetti, S. (1997) 'A survey of telomerase activity in human cancer', *European Journal of Cancer*, 33(5), pp. 787–791.

Shay, J. W. and Wright, W. E. (2000) 'Implications of Mapping the Human Telomerase Gene (hTERT) as the Most Distal Gene on Chromosome 5p', *Neoplasia*, 2(3), pp. 195–196.

Shih, I. M. *et al.* (2001) 'Top-down morphogenesis of colorectal tumors', *Proceedings of the National Academy of Sciences of the United States of America*, 98(5), pp. 2640–5.

Singh, R. *et al.* (2016) 'Sessile serrated adenoma/polyps: Where are we at in 2016?', *World Journal of Gastroenterology*, 22(34), pp. 7754–7759.

Slagboom, P. E., Droog, S. and Boomsma, D. I. (1994) 'Genetic determination of telomere size in humans: a twin study of three age groups', *American journal of human genetics*, 55(5), pp. 876–82.

Spyridopoulos, I. *et al.* (2008) 'Telomere Gap Between Granulocytes and Lymphocytes Is a Determinant for Hematopoetic Progenitor Cell Impairment in Patients With Previous Myocardial Infarction', *Arteriosclerosis, Thrombosis, and Vascular Biology*, 28(5), p. 968-974.

Svenson, U. and Roos, G. (2009) 'Telomere length as a biological marker in malignancy', *Biochimica et Biophysica Acta - Molecular Basis of Disease*, 1792(4), pp. 317–323.

Takagi, S. *et al.* (1999) 'Telomere Shortening and the Clinicopathologic Characteristics of Human Colorectal Carcinomas', *Cancer*, 86, pp. 1431–1436.

Unryn, B. M. *et al.* (2006) 'Acceleration of telomere loss by chemotherapy is greater in older patients with locally advanced head and neck cancer', *Cancer Research*, 12(21), pp. 6345–50.

Valdes, A. M. *et al.* (2005) 'Obesity, cigarette smoking, and telomere length in women', *The Lancet*, 366(9486), pp. 662–664.

Valls, C. *et al.* (2011) 'Telomere length is a prognostic factor for overall survival in colorectal cancer', *Colorectal Disease*, 13(11), pp. 1265–1272.

Vasa-Nicotera, M. *et al.* (2005) 'Mapping of a major locus that determines telomere length in humans', *American Journal of Human Genetics*, 76(1), pp. 147–51.

Vinagre, J. *et al.* (2013) 'Frequency of TERT promoter mutations in human cancers', *Nature Communications*, 4, p. 2185.

Walther, A., Houlston, R. and Tomlinson, I. (2008) 'Association between chromosomal instability and prognosis in colorectal cancer: a meta-analysis', *Gut*, 57(7), pp. 941–950.

Wang, L. *et al.* (2003) 'Association of a functional tandem repeats in the downstream of human telomerase gene and lung cancer', *Oncogene*, 22(46), pp. 7123–7129.

Westphalen, C. B. *et al.* (2014) 'Long-lived intestinal tuft cells serve as colon cancer–initiating cells', *The Journal of Clinical Investigation*, 124(3), pp. 1283–1295.

Willeit, P. *et al.* (2010) 'Telomere length and risk of incident cancer and cancer mortality', *Jama*, 304(1), pp. 69–75.

Wright, W. E. *et al.* (1996) 'Telomerase activity in human germline and embryonic tissues and cells', *Developmental Genetics*, 18, pp. 173–179.

Xia, X. *et al.* (2013) 'MNS16A Tandem Repeats Minisatellite of Human Telomerase Gene and Cancer Risk: A Meta-Analysis', *PLoS ONE*, 8(8), p. e73367.

Zee, R. Y. L. *et al.* (2009) 'Mean telomere length and risk of incident colorectal carcinoma: A prospective, nested case-control approach', *Cancer Epidemiology Biomarkers and Prevention*, 18(8), pp. 2280–2282.

Zheng, R. and Blobel, G. A. (2010) 'GATA Transcription Factors and Cancer', *Genes and Cancer*, 1(12), pp. 1178–1188.

Zusammenfassung

Angesichts der weltweit kontinuierlich hohen Prävalenz und der relativ hohen Mortalität des kolorektalen Karzinoms (KRK) besteht ein großes Interesse, potentielle klinische Biomarker festzustellen, um Hochrisikogruppen für KRK zu identifizieren und folglich den Großteil der Bevölkerung vor einer Koloskopie zu verschonen.
Telomere bestehen aus hoch konservierten Strukturen von Nukleoproteinen, die die Enden der Chromosomen verdecken und verantwortlich für die Erhaltung der Genomstabilität sind, um den Abbau und die Verschmelzung der Chromosomenenden zu verhindern. Es ist weitgehend anerkannt, dass die fortschreitende Verkürzung der Telomere zur genomischen Instabilität beiträgt und wesentlich in den Prozess der Karzinogenese involviert ist. Die Telomerlänge wird durch die humane Telomerase Reverse Transkriptase (hTERT) aufrechterhalten, deren genetische Variationen können möglicherweise die hTERT-Aktivität beeinflussen.

Die vorliegende Masterarbeit ermittelte die Funktionalität von MNS16A, einem „Tandem Repeat" Minisatellit, der „downstream" des hTERT Gens in einer putativen Promotorregion des Antisense-RNA Transkripts von hTERT liegt. Da bisherige Untersuchungen unserer molekularepidemiologischen Forschungsgruppe zwei neue MNS16A Varianten identifiziert hatten, wurde nun die Promotoraktivität aller sechs bekannten MNS16A „variable number of tandem repeats" (VNTRs) in den Kolorektalkarzinom-Zelllinien SW480 und HCT-116 untersucht. Es konnte eine inverse Korrelation zwischen Promotoraktivität und der Anzahl der Tandemwiederholungen gezeigt werden, obwohl Zelllinie HCT-116 ein wesentlich niedrigeres generelles Expressionslevel aufwies. Es bedarf weiterer epidemiologischer Krebsstudien, welche tumortyp- und gewebsspezifische Funktionalität als auch Bindungsstellen für Transkriptionsfaktoren und MNS16A VNTR Länge berücksichtigen, um das Potential der MNS16A Genotypen als Biomarker für Krebsanfälligkeit zu verifizieren.

Im zweiten Teil dieser Arbeit wurde die relative Telomerlänge in Leukozyten des peripheren Blutes (PBL) innerhalb der kolorektalen Krebsstudie von Österreich (CORSA) gemessen, wobei 384 KRK-Fälle als auch 544 Hochrisikoadenome, 537 Niedrigrisikoadenom-Patienten und 546 adenomfreie Kontrollen eingeschlossen wurden, welche alle alters- und geschlechtsangepasst waren. Da vorherige Studien widersprüchliche Assoziationen zwischen KRK und PBL Telomerlänge als potentiellen Biomarker gefunden hatten, umfasste diese

Arbeit zusätzlich prämaligne Vorstufen, um das gesamte Spektrum der putativen KRK Entwicklung zu reflektieren.

Telomere bei Patienten mit KRK waren signifikant länger als bei Kontrollpatienten (*P*-Wert = $3.61x10^{-6}$). Es konnten keine signifikanten Unterschiede weder für Hochriskoadenom-Patienten (*P*-Wert = 0.05956) noch für Niedrigriskoadenom-Patienten (*P*-Wert = 0.05224) festgestellt werden. Eine altersabhängige Verkürzung der Telomere war über die gesamte Studienpopulation hinweg prävalent, obwohl eine Abnahme bei Frauen und Rauchern verstärkt vorlag. Da eine statistisch signifikante Assoziation längerer Telomere bei Patienten mit KRK verglichen mit adenomfreien Kontrollen gefunden wurde, könnte die Telomerlänge in PBL zukünftig als klinischer Biomarker für KRK angewandt werden. Es sind jedoch weitere große Studien notwendig, welche ebenfalls kolorektale Adenome einschließen, um diese Ergebnisse zu bestätigen.